ACS NANOSCIENCE Au
AN OPEN ACCESS JOURNAL OF THE AMERICAN CHEMICAL SOCIETY

pubs.acs.org/nanoau Review

Advances in Inorganic Nanomaterials for Triboelectric Nanogenerators

Renyun Zhang* and Håkan Olin

Cite This: *ACS Nanosci. Au* 2022, 2, 12−31 Read Online

ACCESS | Metrics & More | Article Recommendations

ABSTRACT: Triboelectric nanogenerators (TENGs) that utilize triboelectrification and electrostatic induction to convert mechanical energy to electricity have attracted increasing interest in the last 10 years. As a universal physical phenomenon, triboelectrification can occur between any two surfaces that experience physical contact and separation regardless of the type of material. For this reason, many materials, including both organic and inorganic materials, have been studied in TENGs with different purposes. Although organic polymers are mainly used as triboelectric materials in TENGs, the application of inorganic nanomaterials has also been intensively studied because of their unique dielectric, electric, piezoelectric, and optical properties, which can improve the performance of TENGs. A review of how inorganic nanomaterials are used in TENGs would help researchers gain an overview of the progress in this area. Here, we present a review to summarize how inorganic nanomaterials are utilized in TENGs based on the roles, types, and characteristics of the nanomaterials.

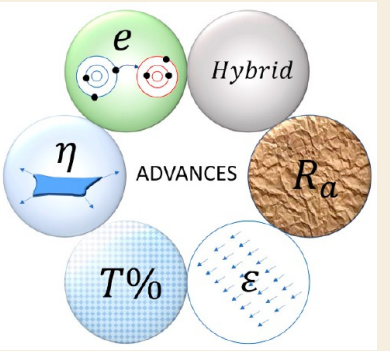

KEYWORDS: *Triboelectric nanogenerators, Nanomaterials, Inorganic nanomaterials*

1. INTRODUCTION

The invention of triboelectric nanogenerators (TENGs) in 2012[1] turned the historic physical phenomenon of triboelectrification (contact electrification)[2] into a working principle for energy conversion. With the development of TENGs, additional applications[3] to energy conversion have been discovered, including sensors,[4−8] control interfaces,[9] functional systems,[10] and biomedical applications.[11,12] The nature of triboelectrification implies that it can occur between any two materials that have physical contact and separation, as charges can transfer between the surfaces. For this reason, diverse materials have been studied for use in TENGs with different purposes, utilizing unique physical and chemical properties.

There are many review articles[13−24] that have described the working modes, mechanisms, and applications of TENGs. Zheng et al. have reviewed the application of TENGs in biomedical applications.[13] Chen and co-workers[14] and Wang et al.[20] have reviewed energy harvesting and self-powered sensing using TENGs. Wang[15,16] has reviewed the theoretical progress of triboelectrification. Zhang and Olin[17] and Bai et al.[19] have reviewed the materials that are utilized in TENGs. Pan and co-workers[25] have reviewed the applications of TENGs for future soft robots and machines. In this Review, we skip this part of the information and focus solely on how inorganic nanomaterials are used to improve the performance of TENGs.

The performance of TENGs is highly dependent not only on the triboelectric materials and their dielectric properties but also on how to pair two triboelectric materials. With the aim of boosting performance, nanomaterials have been introduced to TENGs. Nanomaterials can serve as either electrode or triboelectric materials, depending on the types of nanomaterials and how they are utilized. Nanomaterials in all dimensions have been applied to TENGs with significant performance improvements.

This Review summarizes the utilization of nanomaterials via several aspects: (1) the roles of inorganic nanomaterials, (2) the types of inorganic nanomaterials, and (3) the composition of the nanomaterials. Perspectives of future studies are also given after the summary. This Review provides an overview of how inorganic nanomaterials that are used in TENGs can lead to further development in this area.

2. THE ROLES OF INORGANIC NANOMATERIALS IN TENGs

The roles of nanomaterials can be divided into two categories: electrode materials and triboelectric materials. Metallic nanomaterials and some carbon-based nanomaterials have been

Received: September 14, 2021
Revised: October 11, 2021
Accepted: October 12, 2021
Published: October 27, 2021

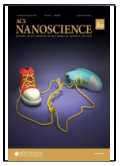

https://doi.org/10.1021/acsnanoscienceau.1c00026
ACS Nanosci. Au 2022, 2, 12−31

used as electrode materials in TENGs because of their excellent electrical properties.

The differences in physical and chemical properties of the triboelectric materials place great importance on electrode selection. The most common nanomaterials used as electrode materials are thermally evaporated gold[26] or copper[27] nanofilms at the backside of triboelectric materials. Such deposited nanofilms have a larger contact area (Figure 1) between the

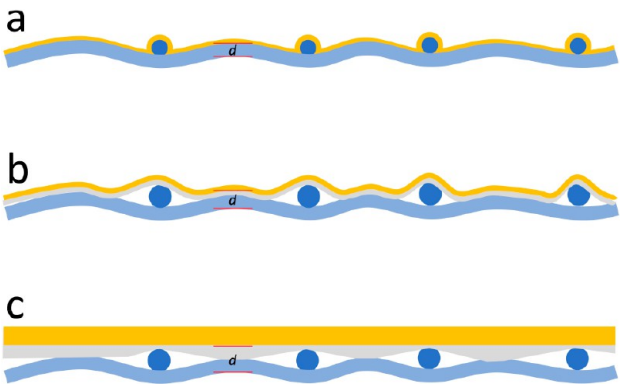

Figure 1. Different electrodes have been used in TENGs. (a) Thermally evaporated metallic nanofilms, (b) glue-based electrode attachment, and (c) metallic tape-based electrode attachment. The *d* in the figure shows the electrostatic induction distance of the TENGs.

electrode and the triboelectric material, which can enhance electrostatic induction. These nanofilms are of critical importance when materials with high roughness such as textiles[28] are used as triboelectric materials. Glue- or tape-based electrode attachment methods (Figure 1) limit the contact area between the electrode and the triboelectric surfaces. Moreover, the direct deposition of a nanofilm eliminates the glue layer, which reduces the distance of electrostatic induction, resulting in a higher current output for the TENGs.

In addition to metallic materials,[29] carbon materials such as graphene[30] have also been used as electrodes in TENGs due to their excellent electrical conductivity, flexibility, and optical properties. Different techniques have been used to produce graphene, including chemical vapor deposition (CVD),[27,30−33] laser induction,[34,35] layer-by-layer assembly,[36] and doping.[37] Carbon nanotubes[31,32,38−40] have also been applied as electrodes in different forms. Carbon nanotubes could serve as pure electrodes in the form of network layers or be embedded in polymers[38−40] to enhance the flexibility of the TENGs.

The utilization of inorganic nanomaterials to improve the performance of TENGs has gained the most interest from researchers. The reasons are as follows: (1) surfaces with inorganic nanomaterials have different charge distributions on flat surfaces; (2) the high surface energy of inorganic nanomaterials can enhance the charge transfer between triboelectric surfaces; (3) the dielectric properties of inorganic nanomaterials can change the properties of composites containing inorganic nanomaterials; and (4) nanomaterials can bring extra characteristics to TENGs that can promote their application in specific areas. Of course, there are other advantages that nanomaterials have brought to TENGs. We review the utilization of inorganic nanomaterials below.

3. INORGANIC NANOMATERIALS USED IN TENGs

Inorganic nanomaterials that have been studied in TENGs include metallic nanomaterials, metallic oxides, 2D materials, perovskites, ferroelectric nanomaterials, and carbon nanomaterials. The utilization of these nanomaterials is due to their electrical, dielectric, and surface topographical properties; e.g., metallic nanomaterials have good conductivity, metallic oxides such as TiO_2 have strong positive charge affinities, 2D semiconductors have flat surfaces and mechanical flexibilities, and ferroelectric nanomaterials can provide piezoelectricity.

3.1. Metallic Nanomaterials

3.1.1. Gold Nanomaterials. Gold nanofilms are commonly used metallic nanomaterials as electrodes in TENGs due to their excellent conductivity and low contact resistance. In addition to the direct thermal deposition methods reviewed above, a sputter coat of gold on a prestretched elastomer film could result in a crumpled gold electrode.[41] Such a crumpled electrode (Figure 2a) could increase the contact area between the gold and the countertriboelectric layer. Such an advance has led to a maximum open-circuit voltage of 124.6 V, a maximum current of 10.13 μA, and a power density of 0.22 mW/cm^2. The same increment of contact area has also been found on nanoflowers (Figure 2b), similar to gold electrodes deposited by electrochemical methods.[42] The top performances of the TENG are 110 V, 5.5 μA, and 150 μW/cm^2.

Different from the gold nanofilms reviewed in the above section, where the films are used only as electrodes, gold nanofilms have also been used as triboelectric layers.[26] The reasons metallic films are used as both triboelectric layers and electrodes are their excellent electric conductivity, high permittivity, and charge affinity.[17] The presence of gold nanoparticles could increase the contact area[43] with the counterlayer, such as polymers, and enhance the stability of the output due to the high oxidation resistance of gold. The output power of a TENG (Figure 2c) in the presence of a 56 nm gold nanoparticle layer was enhanced 25 times[44] due to the increase in contact area and nature of the positively charged gold nanoparticle surfaces. An area power density of 313 W/m^2, a volume power density of 54 268 W/m^3, and a maximum open-circuit voltage of 1200 V were obtained on the TENG.

In addition to the nanofilms, gold nanoparticles have also been impregnated in PDMS mesoporous pores[45] and served as triboelectric layers to generate charges with a PDMS (Figure 2d). The impregnation of gold nanoparticles enhanced the power of TENGs over 5-fold compared to a flat film. Similar to this impregnation process, gold nanosheets have been embedded in a PDMS film[46] to enhance the stability and stretchability of TENGs (Figure 2e) and in a PTFE film to enhance the surface charge density and the output current.[47] The stretchability of TENGs brought by the gold nanosheet allows them to be applied at the joints of the human body for energy harvesting and sensing. Tactile sensors have been made with embedded gold nanostructures[48] with potential application in human−machine interactions (Figure 2f).

Table 1 summarizes the performances of the gold nanomaterial constituted TENGs, showing the nanomaterials, countertribolayers, open-circuit voltages, short current or current densities, and power densities.

3.1.2. Silver Nanomaterials. Silver is another widely used metallic material in TENGs. Compared to silver nanoparticles, silver nanowires are more commonly used in TENGs. Silver nanowires are popular because they can be simply transformed

https://doi.org/10.1021/acsnanoscienceau.1c00026
ACS Nanosci. Au 2022, 2, 12−31

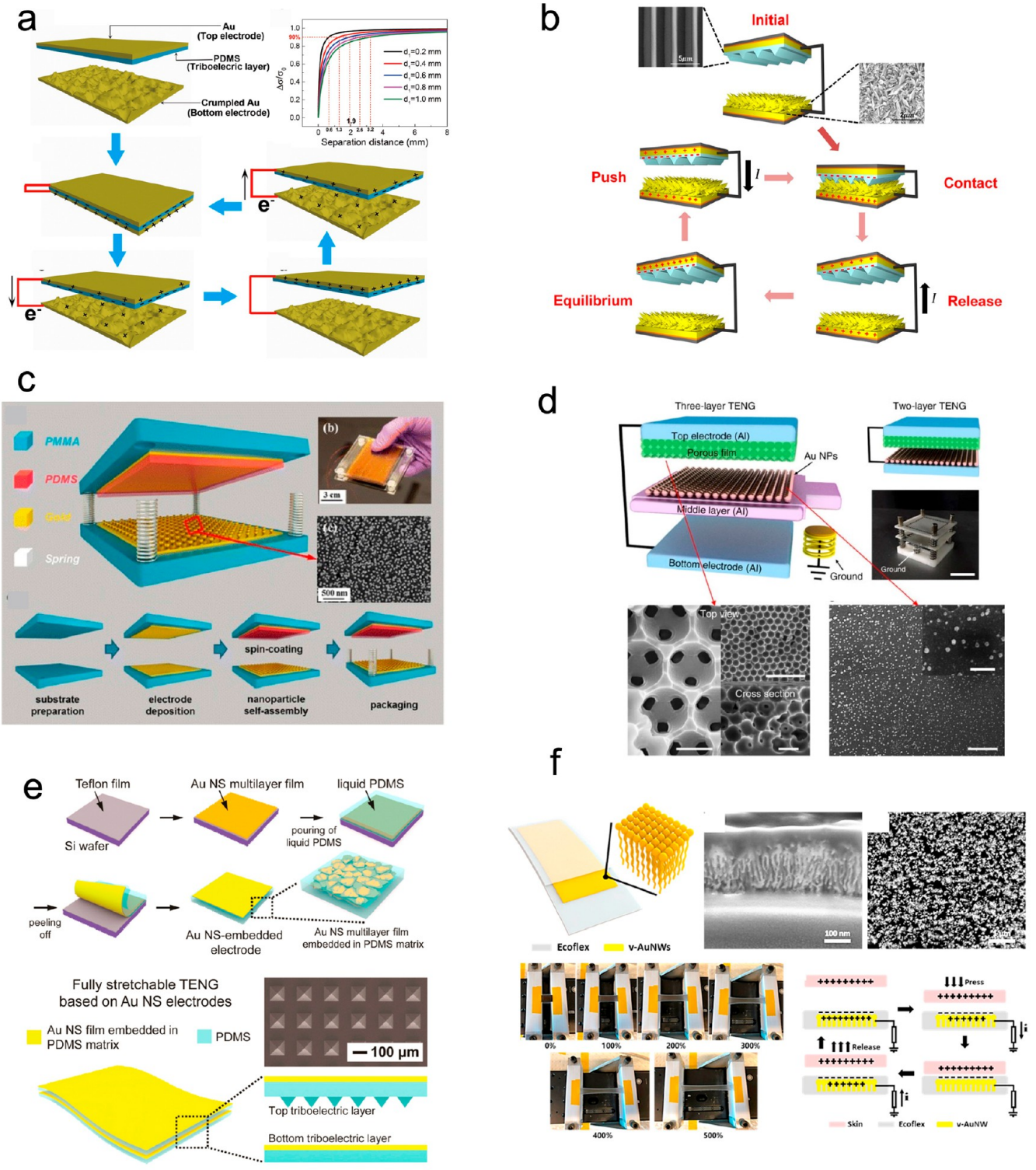

Figure 2. Gold nanomaterial constituted TENGs. (a) Crumpled gold film-based TENG. Reproduced from ref 41. Copyright 2018 Elsevier. (b) Gold nanoflower-based TENG. Reused under CC BY 4.0 (ref 42). (c) Gold nanoparticle-based TENG. Reproduced from ref 44. Copyright 2013 American Chemical Society. (d) Gold nanoparticle-based TENG. Reused under CC BY 4.0 (ref 43). (e) Embedded gold nanosheet-based TENG. Reproduced from ref 46. Copyright 2017 Elsevier. (f) Gold nanowire-based TENG. Reproduced from ref 48. Copyright 2020 Elsevier.

into transparent, flexible, and low-resistance electrodes for use in TENGs. Another reason is that the methods for the synthesis of silver nanowires are generally simple. Table 2 summarizes the performances of the silver nanomaterial constituted TENGs.

Yang's group reported a silver nanoparticle film-based TENG[49] for harvesting energy from wind, where a silver nanoparticle film pasted on photograph paper was used as both an electrode and a triboelectric material. The positive charge affinity nature of the silver nanoparticles offers a rapid charging and discharge process and thus high output performance for a

https://doi.org/10.1021/acsnanoscienceau.1c00026
ACS Nanosci. Au 2022, 2, 12−31

Table 1. Performances of gold Nanomaterial Constituted TENGs

gold nanostructures	counter tribolayer	open-circuit voltage (V)	current or current density	power density (mW/cm^2)	ref
crumpled gold film	PDMS	124.6	6.75 μA/cm^2	0.22	41
gold nanoflower	PDMS	110	1.53 μA	0.15	42
gold nanoparticles	PDMS	300	1.22 mA	46.8	43
gold nanoparticles	PDMS	~1200	2 mA	313	44
gold/pdms	Al	150	0.62 μA/cm^2	0.16	45
gold nanosheets	PDMS	60	2.8 μA		46
gold nanowire	skin	0.1−0.2			48

Table 2. Performances of Silver Nanomaterial Constituted TENGs

silver (Ag) nanostructures	counter tribolayer	open-circuit voltage (V)	current or current density	power density (mW/cm^2)	ref
Ag nanoparticles	FEP	200	20 μA	0.11	49
Nano-Ag ink	Kapton	160	6.6 μA/cm^2	1.2 mW/cm^3	50
Ag NW	Al/Skin	66	8.6 μA	0.0446	49
Ag/PEDOT:PSS	PUA	170	50 μA	1.5	50
Ag NW	FEP	150	7.5 μA	0.036	54
Ag NW/PDMS	PFA	120[a]	22 μA[a]		55
	Nylon	18[a]	3.5 μA[a]		
Ag NW (as a transparent electrode)		3600	7 μA		56
Ag NW (as an electrode)		330	15.5 μA	0.25	57
Ag NW/PVDF	Nylon	240	12 μA[a]		58

[a]Data read from the figures in the paper.

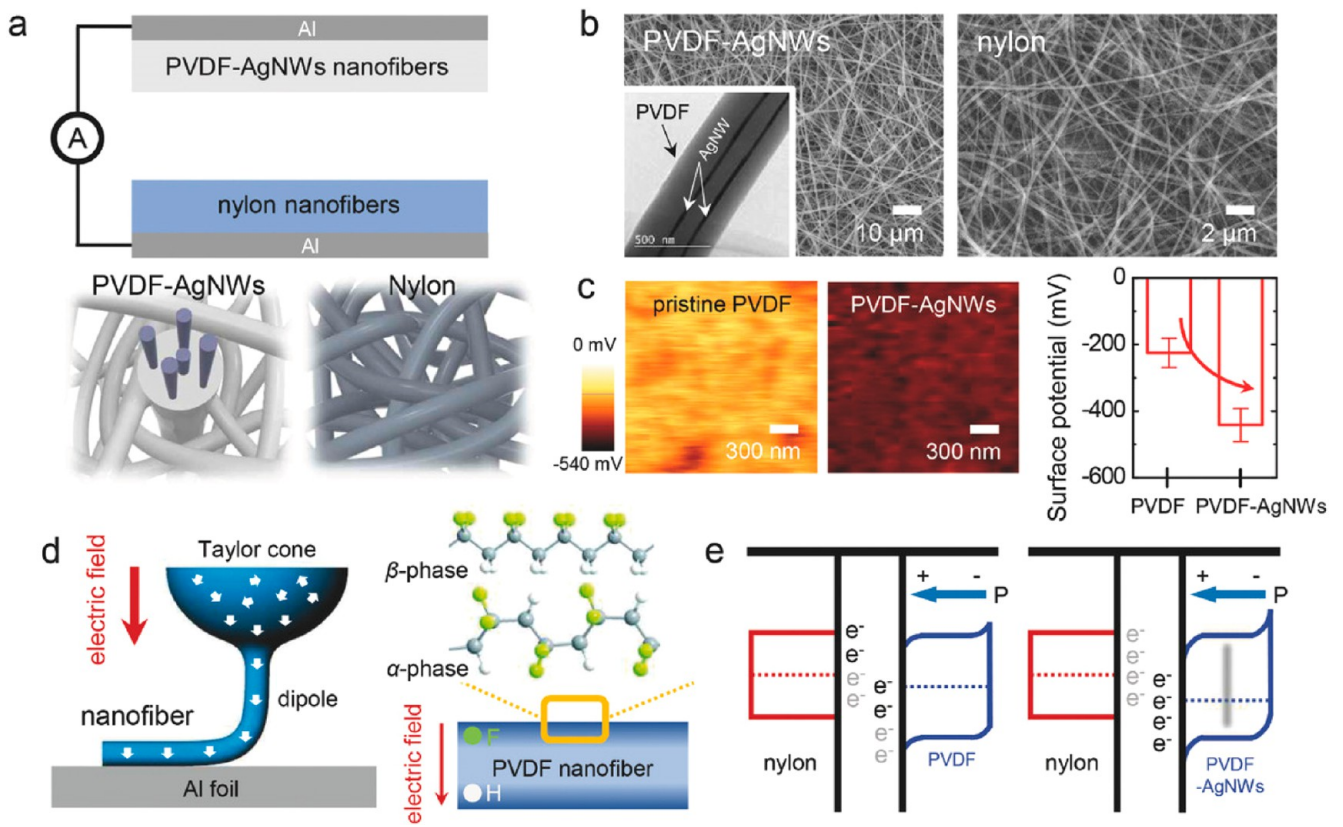

Figure 3. (a) Schematic diagrams of the TENGs based on the PVDF−AgNW composite and nylon nanofibers prepared by electrospinning methods. (b) SEM images of the electrospun PVDF−AgNW composite and nylon nanofibers. The inset shows a TEM image of the PVDF−AgNW composite nanofibers. (c) KPFM images of the surfaces of the pristine PVDF and PVDF−AgNW composite nanofibers. The right panel shows the surface potentials of the nanofibers. (d) Schematic illustration of the electrospinning process applied to a PVDF solution. (e) Schematic band diagrams explaining the TENG operation mechanism. Reproduced from ref 58. Copyright 2020 Wiley-VCH Verlag.

TENG. Brushing nanosilver ink[50] on photopaper has also been used to create a silver film for use in TENGs.

Although the enhancement of silver nanoparticles has been proven, more studies have utilized silver nanowires since more features, as described above, could be created. Example

https://doi.org/10.1021/acsnanoscienceau.1c00026
ACS Nanosci. Au 2022, 2, 12−31

Table 3. Performances of Metallic Oxide Constituted TENGs

metallic oxide	counter tribolayer	voltage (V)	current	power	ref
ZnO	PI	31.6	5.43 μA		63
ZnO (Ga-doped)	PDMS	27	119 nA/cm^2		64
ZnO (Sb-doped)	Nylon	12	110 nA/cm^2		60
ZnO	PTFE	28	4.5 μA	80 μW/cm^2	61
ZnO	Ag	120	65 μA	1.1 mW[a]	65
ZnO/MWCNT/PDMS	Al	140.81	6.10 μA	0.26 W/cm^2	67
ZnO	PI	80	0.9 μA[b]	1.12 W/m^2	68
ZnO	PTFE	57	59 mA/m^2	1.1 W/m^2	69
ZnO/BC	Teflon	57.6	5.78 nA	42 mW/m^2	70
ZnO/PVDF	PTFE	119	1.6 μA	10.6 μW/cm^2	71
TiO_{2-x}/PDMS	PDMS	180	8.15 μA	1.84 W/m^2	75
TiO_2/rubber	PTFE	113	9.8 μA	237 mW/m^2	76
Fe_3O_4/PVDF	Al	138	5.68 μA		82

[a]Four layer stacked. [b]Data read from the figure in the paper.

features are the flexibility and transparency of silver nanowire-based electrodes.[51] These features are of great importance for the application of TENGs as sensors to be attached to the human body.[52,53]

Pasting,[54] spin coating,[52] Meyer-rod coating,[55] and splashing[56] are commonly used methods for creating silver nanowire electrodes, as these methods allow easy control of the thickness of silver nanowire films. To improve the performance of the electrodes, an embedding technique[57] has been used to fix the silver nanowire networks inside polymers such as PDMS,[46] PVDF (Figure 3),[58] and PEDOT:PSS[53] so that the contacts among the silver nanowires will not be lost during physical deformation. The embedding of the silver nanowires maximizes the contact between the polymer, which enhances the electrostatic induction of the TENGs. To further increase the stability of the performance of the TENGs, researchers welded silver nanowires[52,59] before embedding.

3.2. Metallic Oxides

Metallic oxides such as TiO_2 and ZnO have high positive charge affinities, making them easy to pair with materials with negative charge affinities. The tunable surface morphologies and the work functions of these materials can ultimately affect the electrical performance[61] of TENGs. In addition, the permittivity of the metallic oxides[62] could also have an impact on the charge transfer process of the TENGs. Table 3 summarizes the performances of some of the TENGs constructed with metallic oxides.

3.2.1. ZnO Nanomaterials. The tunable surface morphologies of ZnO make it possible to design specific structures for TENGs. Nanoparticles,[63] nanorods,[60,61,64−66] nanoflowers,[67] nanoripples,[68] and microballon arrays[69] have been created and used in different TENGs. The open-circuit voltage of TENGs using ZnO nanostructures is usually lower than 100 V,[61,63,64,70] while the number can be improved to above 100 V[71] to several hundred volts[72] if specifically composited with polymers.

One unique feature of using ZnO nanomaterials is that one can dope the materials to change their electrical behaviors. A TENG performance boosting effect can be brought by charge transfer at the surface due to doping.[60] Chen et al. reported that 4 M % Sb-doped ZnO nanorod arrays can boost the output voltage and current by 24 and 5.5 times compared to undoped arrays. Sb doping bends the band of the ZnO nanorod arrays downward (Figure 4), leading to more electrons being transferred to the countertriboelectric surface.

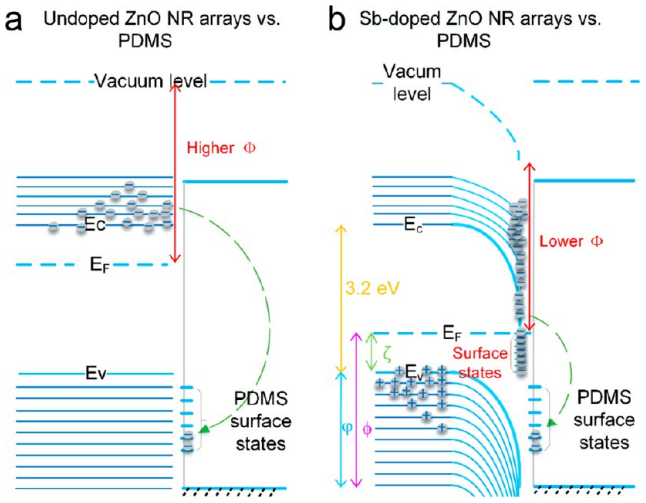

Figure 4. Proposed possible surface energy downward bending diagrams and tribocharge transfer for the TENG made of (a) undoped ZnO NR arrays and (b) Sb-doped ZnO NR arrays against PDMS before contact. Reproduced from ref 60. Copyright 2018 Elsevier.

A similar phenomenon has also been found on Ga-doped ZnO nanorod arrays.[64] Another TENG performance boosting effect brought by doping is the high trap density close to the conduction band edge, which results in shallow trapped electrons.[73]

3.2.2. TiO_2 Nanomaterials. Similar to ZnO, TiO_2 nanomaterials have tunable shapes and sizes. TiO_2 nanoparticles[74−77] have been more widely studied in nanogenerators. In most studies, TiO_2 nanomaterials are embedded[75] or composited[74] with polymers to improve the TENG performance. The chemical modification of TiO_2 nanostructures[78] is another way to enhance the output of TENGs.

The high dielectric constant of TiO_2 nanomaterials is one of the factors that improves the output performance of TENGs. Moreover, the oxygen vacancies[79,75] in TiO_2 composites have also been suggested as a factor of performance enhancement.

3.2.3. Other Metallic Oxides. In addition to ZnO and TiO_2, other metallic oxide nanomaterials, such ITO,[80] Al_2O_3,[81] and Fe_3O_4,[82] have also been studied for their applications in TENGs. Chun et al.[80] reported a TENG based on an interlocked array of surface-functionalized ITO nanohelixes

https://doi.org/10.1021/acsnanoscienceau.1c00026
ACS Nanosci. Au 2022, 2, 12−31

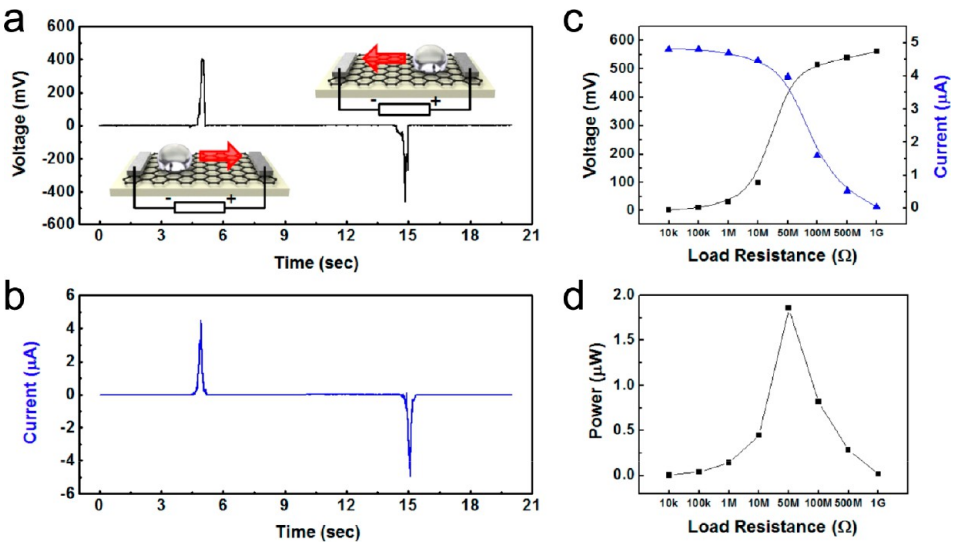

Figure 5. Water droplet-based electric power generation from a graphene/PTFE structure. (a) Voltage output from a graphene/PTFE structure by a single moving droplet of 0.6 M NaCl on a graphene surface with a reversed voltage signal output of a graphene/PTFE structure obtained by reversing the moving direction of the droplet. (b) Current output from the graphene/PTFE structure according to the forward and reverse motion of the water. (c, d) Dependence of the output voltage and current as a function of the external load resistance and corresponding maximum power output by a single moving droplet of 0.6 M NaCl, respectively. Reproduced from ref 87. Copyright 2016 American Chemical Society.

and demonstrated an over 340 times output enhancement compared to a flat ITO. Such enhancement is attributed to the nanoscale roughness, negligible degradation against external force and strain, and efficient charge generation and induction. Kim's group reported a stoichiometric Al_2O_3-based TENG[81] that reveals meaningful electric power generation under mechanical friction.

3.3. 2D Nanomaterials

The application of 2D nanomaterials has gained increasing attention from researchers due to their unique geometry and electrical and dielectric properties. Based on the difference in electrical and dielectric properties, 2D nanomaterials have been used as electrodes or triboelectric layers in TENGs.[83]

3.3.1. Graphene and Graphene Oxide. Graphene is a monolayer of carbon atoms that exhibits excellent electrical conductivity. Such a property makes graphene a good alternative to metallic electrodes. Moreover, graphene is an inert material that makes it chemically stable under extreme conditions. The transparency of graphene brings more features to TENGs. From a sustainable perspective, graphene is a green material that can benefit the development of environmentally friendly TENGs.

Shankaregowda et al.[84] reported a flexible and transparent TENG based on a graphene layer grown by a CVD method, in which graphene was used as both an electrode and a triboelectric layer. Such a TENG has maximum outputs of 650 V, 12 μA, and 0.21 mW/cm^2. By crumpling the graphene layer,[85] the output power density can reach 0.25 mW/cm^2. By aligning the graphene sheets,[86] the output power density reached 4.8 mW/cm^2. The alignment of the graphene sheets forms numerous microcapacitors and has a low dielectric loss that contributes to a high output power density.

A graphene layer has also been applied to convert mechanical energy from water droplets. Kwak et al.[87] reported a triboelectrification-induced large electric power generator based on a graphene/PTFE structure (Figure 5). The transfer of graphene on the PTFE surface polarized the graphene with negative charges accumulated on the top surface that interacted with the droplet to generate electricity. An output power of 1.9 μW from a single droplet was measured based on the unique graphene/PTFE structure.

Although CVD-grown graphene has excellent electrical conductivity, the production rate is still quite low due to the limitation of the technique. Alternatively, researchers have used reduced graphene oxide (rGO) in the development of TENGs. Usually, rGO is produced using thermal[88,89] and optical[34] methods. rGO can be used as either electrodes or triboelectric layers, depending on the design. Stanford et al.[34] and Zhao et al.[35] reported two separate studies on laser-induced graphene as electrodes. The first group used a 75 W pulse laser, while the second group used an 8.1 W continuous laser. Li et al.[90] reported a TENG using thermally reduced rGO at 700 °C as a triboelectric layer and successfully converted the mechanical energy between the rGO and electrolyte into electricity. Zhao and co-workers[88] reported a foam structure made from thermally reduced rGO and polyimide (PI) and used it as a pressure-sensitive electrode in a wind-driven TENG. Wu et al.[91] reported the electron-trapping behavior of rGO embedded in a PI film, which can enhance the output approximately 30 times.

In some cases, GO has not been reduced for use in a TENG. Harnchana et al. reported a TENG made from a composite of GO, PDMS, and SDS[92] that has an output of 438 V and 11 μA/cm^2. Such performances are approximately three times those of a flat PDMS layer. GO can also be used directly as a triboelectric layer[93] for energy harvesting and dynamic force sensing. Such a simple construction enabled the TENG to have a surprisingly high performance, with a short-circuit current density of 3.43 μA/cm^2, an open-circuit voltage of 1100 V, and a power density of 3.13 W/m^2. Moreover, the TENG can also act as a force sensor with a sensitivity of 388 μA/MPa.

3.3.2. MXenes. MXenes are a class of 2D transition metal carbides, carbonitrides, and nitrides with compositions of $M_{n+1}AX_n$. MXenes are electronegative materials owing to their electric negative surface groups such as −OH and −F, making them candidate triboelectric materials for use in TENGs.[95]

https://doi.org/10.1021/acsnanoscienceau.1c00026
ACS Nanosci. Au 2022, 2, 12−31

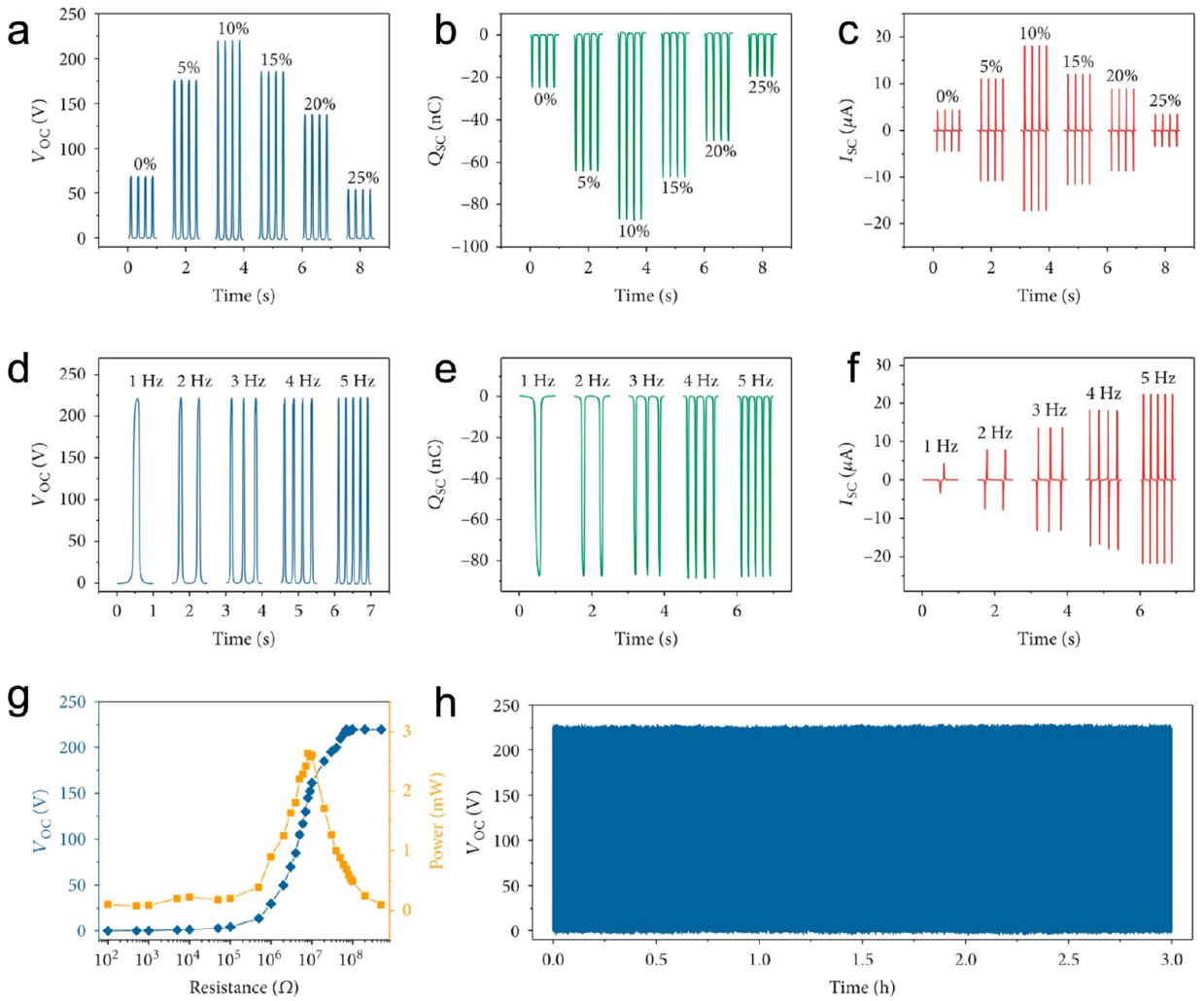

Figure 6. Triboelectrification of the MXene/PVDF membrane. (a–c) Open-circuit voltage (a), short-circuit transferred charges (b), and short-circuit current (c) of the TENG based on the MXene/PVDF membrane at different loadings ranging from 0% to 25%. (d–f) Open-circuit voltage (d), short-circuit transferred charges (e), and short-circuit current (f) of the TENG at an MXene loading of 10% operated at different frequencies (1–5 Hz). (g) Dependence of the output performance of the TENG on the external loadings. (h) Stability test of the fabricated TENG based on the MXene/PVDF membrane. Reference 94, reused under CC BY 4.0.

Reports have indicated that MXenes can be more negative than PTFE.[96]

Due to the strong electronegativity of MXenes that attract electrons during triboelectrification processes, the open-circuit voltage of TENGs based on MXenes is usually high. For example, a TENG with a structure of MXene/glass:PEI-ITO[97] can have an open-circuit voltage of 650 V. However, the output power density was found to be approximately 0.05 mW/cm^2, which could be improved. To improve the performance of TENGs, researchers have composited MXenes with or embedded in polymers. The presence of MXenes in polymer films has two effects, dielectric permittivity and percolation, that need to be balanced by the percentage of MXenes (Figure 6) to obtain the maximum performance.[94]

PDMS is one of the most commonly used polymers to composite with MXenes.[98−101] Liu et al. reported a PDMS/MXene (4:1) triboelectric layer for use in TENGs[99] that can achieve outputs of 453 V and 132 μA. He and co-workers[98] studied different compositions of PDMS/MXene where the weight concentration of the MXene was tuned between 1% and 5%. TENGs fabricated with a spin-coated PDMS/MXene triboelectric layer can achieve an output power density of up to 10 mW/cm^2.

Fluoropolymers such as PTFE,[96] PVDF-TrFE,[103] and PVDF[94,106] have also been used in composites with MXenes. Theoretical analysis was reported by Zhang et al.,[105] who indicated that the percentage of MXenes in the PVDF film can be tuned to maximize the output. Experimentally, 10% MXene in the PVDF film provided an output of 0.22 mW/cm^2. The same percentage of MXene has also been reported by Bhatta et al.[106] where PVDF fibers were functionalized by10% of MXene. An output of 1.1 mW/cm^2 was obtained on the TENG operated in contact-separation mode.

Other polymers, such PVA,[107,108] rubber,[104] and PDOT:PSS,[105] have also been used in composites with MXenes for use in TENGs. An output power density of 0.11 mW/cm^2 has been reported[109] based on a triboelectric layer of PVA/MXene fibers with 30 vol % MXene. In another report,[108] 4 wt % MXene revealed the best performance.

In addition to the composition with polymers, MXenes can also be composited inorganic materials for use in TENGs. Feng and co-workers[110] reported an alternate-layered MXene composite produced with Nb_2CT_x and Ti_3CT_x. They found

https://doi.org/10.1021/acsnanoscienceau.1c00026
ACS Nanosci. Au 2022, 2, 12−31

Table 4. Performances of MXene Constituted TENGs

MXene (or composites)	counter tribolayer	voltage (V)	current	power	ref
MXene/PTFE	Cu	397	21 μA	0.09 mW/cm^2	96
MXene	PET	650	7.5 μA	0.65 mW	97
3D MXene/PDMS	Nylon	45	0.6 μA		95
MXene/PDMS	PET	80[a]			101
MXene/PDMS	PDMS	453	131 μA		99
MXene/PDMS	Skin	225	30 μA/cm^2	10 mW/cm^2	98
PVDF-TrFE/MXene	Nylon	270	140 mA/m^2	4.02 W/m^2	103
PVDF/MXene	Nylon	724	163.6 μA	11.213 W/m^2	100
MXene/PVA	Kapton	230	270 nA	0.33 W/m^2	102
MXene/Ecoflex	Nylon	790	183 μA	9.24 W/m^2	104
MXene-PDOT:PSS	PTFE	29.56			105

[a]Data read from the figures in the paper.

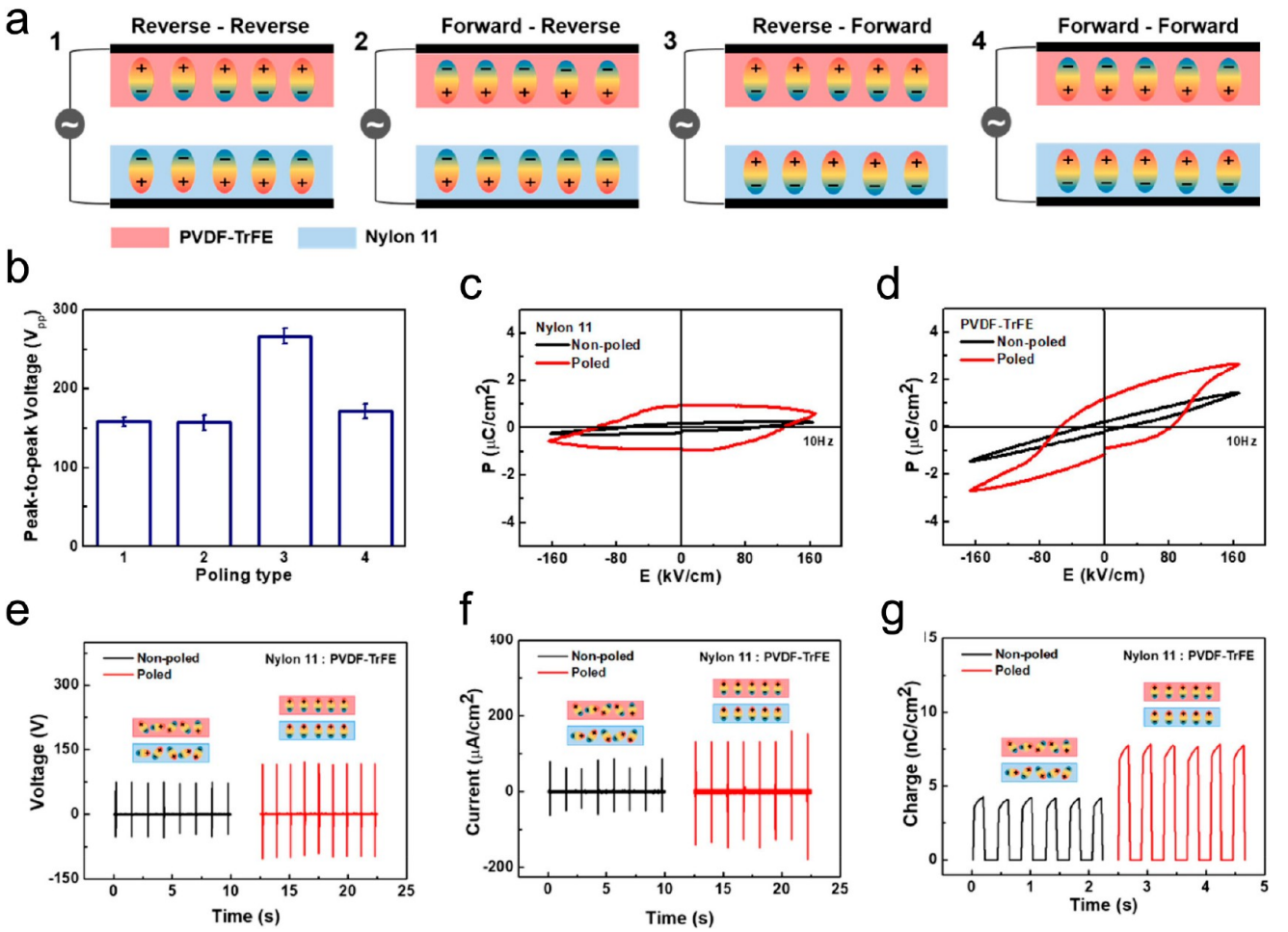

Figure 7. (a) Schematic drawings of four different polarization pairs. (b) Comparison of the output peak-to-peak voltages for each poling pair. (c) *P*–*E* curves of nonpoled nylon-11 and poled nylon-11. (d) *P*–*E* curves of nonpoled PVDF-TrFE and poled PVDF-TrFE. The enhancement in (e) output voltage, (f) current density, and (g) charge density before (black colored line) and after (red colored line) polarization of the friction surfaces. Reproduced from ref 102. Copyright 2019 American Chemical Society.

that 15 wt % Nb_2CT_x in the composite could lead to the best performance of the TENGs.

The electrical conductivity of MXenes makes them not only good triboelectric materials but also alternative electrodes in TENGs. Cao et al.[111] produced a type of MXene liquid electrode for improving the performance of a TENG working in a single electrode mode. Enhanced outputs up to 300 V and 0.37 μA/cm^2 were achieved.

A summary of the performances of the TENGs made of MXenes and composites is given in Table 4.

3.3.3. 2D Semiconductors. 2D semiconductors used in TENGs are mostly transition metal dichalcogenide (TMD) materials, including MoS_2, WS_2, $MoSe_2$, and WSe_2. The use of these 2D materials could benefit the theoretical understanding of the mechanism of triboelectrification. Seol and co-workers[83] made a triboelectric series of 2D layer materials and pointed out that the triboelectric effects of the 2D studied triboelectric

https://doi.org/10.1021/acsnanoscienceau.1c00026
ACS Nanosci. Au 2022, 2, 12–31

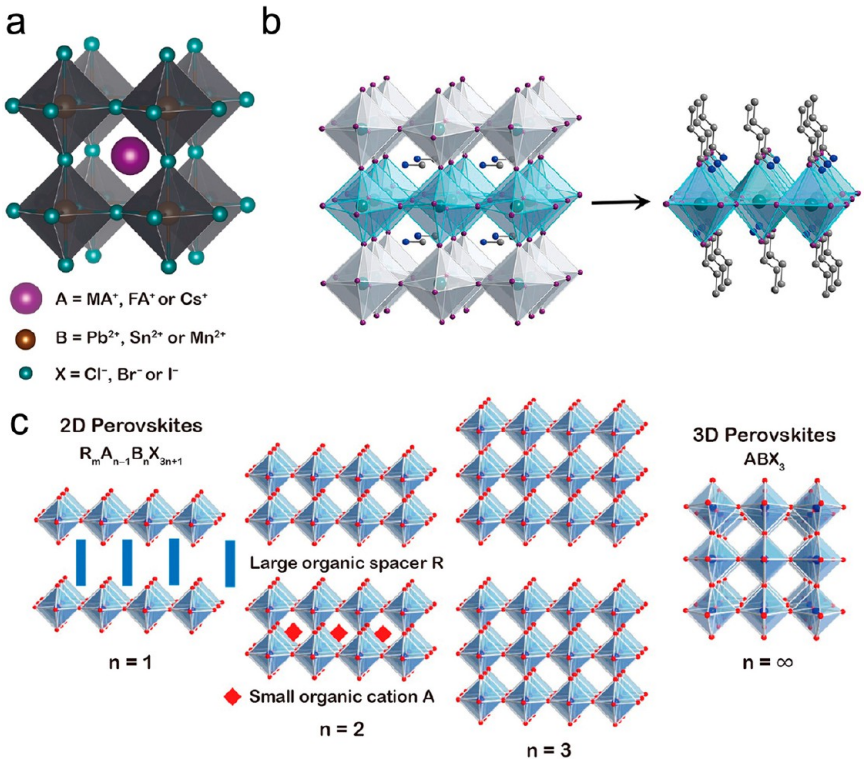

Figure 8. (a) Schematic representation of the typical 3D perovskite structure ABX_3. A cation is adopted into the body center of the cubic structure formed by eight corner-sharing $[BX_6]^{4-}$ octahedra. (b) Schematic representation of a 3D perovskite $MAPbI_3$ sliced into a 2D perovskite $(C_4H_9NH_3)_2PbI_4$ along the (001) crystallographic plane. (c), Structures of the 2D perovskites of $R_mA_{n-1}B_nX_{3n+1}$ (from $n = 1$ to $n = \infty$) in different numbers of inorganic metal-halide layers. Reference 117, reused under CC BY 4.0.

materials are obviously related to the effective work functions. According to the maximum output voltage and current, the 2D materials can be listed in the order of (−) MoS_2, $MoSe_2$, WSe_2, and WS_2 (+).

Among these 2D semiconductors, MoS_2 is the most investigated in TENGs. MoS_2 materials can act solely[112,113] as a triboelectric layer for energy conversion or be composited with other polymers.[114−116] The output power densities of the MoS_2 constituted TENGs range from 74 nW/cm^2 to 50 mW/cm^2, while the open-circuit voltage ranges from 2.3 to 145 V. The highest output, 50 mW/cm^2, is from a TENG[102] with both triboelectric layers composited with MoS_2 flakes and polarized afterward (Figure 7).

The unique semiconductive property of MoS_2 leads to different electrical contacts in the TENGs. In some cases,[116] the depletion layers that formed between MoS_2 and other materials, such as Au and PPy, could enhance the output of the TENGs. This mechanism can have an impact on other 2D semiconductors but needs further study.

3.4. Perovskites/Ferroelectric Nanomaterials

Perovskites (Figure 8) have recently gained much attention due to their successful applications[117] in energy harvesting technologies, including solar cells and TENGs. Recently, Ippili et al.,[118] have reviewed the progress of the halide perovskite-based triboelectric self-powered sensors, showing the great potential of the materials. In most of the studies, single crystalline system of perovskites have been utilized, while the binary crystalline system of perovskites remains are less focused.

Many perovskites are also ferroelectric. In some papers, perovskites are emphasized, while others emphasize ferroelectricity. Therefore, we created a combined section for perovskites and ferroelectric nanomaterials.

Originally, perovskite refers to calcium titanate ($CaTiO_3$). Recently, it refers to the class of compounds that have the same type of crystal structure, $^{XII}A^{2+VI}B^{4+}X^{2-}{}_3$. The "A" in the form can be either metals or organic groups. However, more perovskite structures have been synthesized recently that have different formulas, where "B" can combine two or more elements, such as $Sr_3Co_2WO_9$.[119]

3.4.1. Lead Halide Perovskites. The organolead halide perovskite $MAPbI_3$ was first used in a triboelectric photodetector in 2015.[120] Taking advantage of the excellent light absorption capability[121] of $MAPbI_3$, enhanced performance has been achieved on a TENG, where the open-circuit voltage, short-circuit current, and amount of electric charge have been increased by 11%, 11%, and 9%, respectively. The output increase was further improved by using a hybrid perovskite structure,[122] $MAPbI_xCl_{3-x}$. The structure couples the triboelectric and photoelectric conversion mechanisms and realizes enhancements of 55.7%, 50.8%, and 58.2%. Although the advantages of organolead halide perovskites in TENGs have been demonstrated in these studies, the output, especially the power density, remains modest.

The performance of TENGs has recently been improved by using inorganic lead halide perovskites, such as $CsPbBr_3$,[124] $CsPbBr_{2.6}I_{0.4}$,[125] $Co(OH)(CO_3)_{0.5}$/Pt/$CsPbIBr_2$,[126] and Ba^{2+}-doped $CsPbBr_3$.[127] It seems that $CsPbBr_3$ has the best performance in TENGs with or without doping compared to the other perovskites. In the case of doping, the electron binding energy, surface potential, and dielectric property of $CsPbBr_3$ can be optimized to obtain the best performance. For example, a TENG[127] made of $CsPb_{0.91}Ba_{0.09}Br_3$ resulting from

https://doi.org/10.1021/acsnanoscienceau.1c00026
ACS Nanosci. Au 2022, 2, 12−31

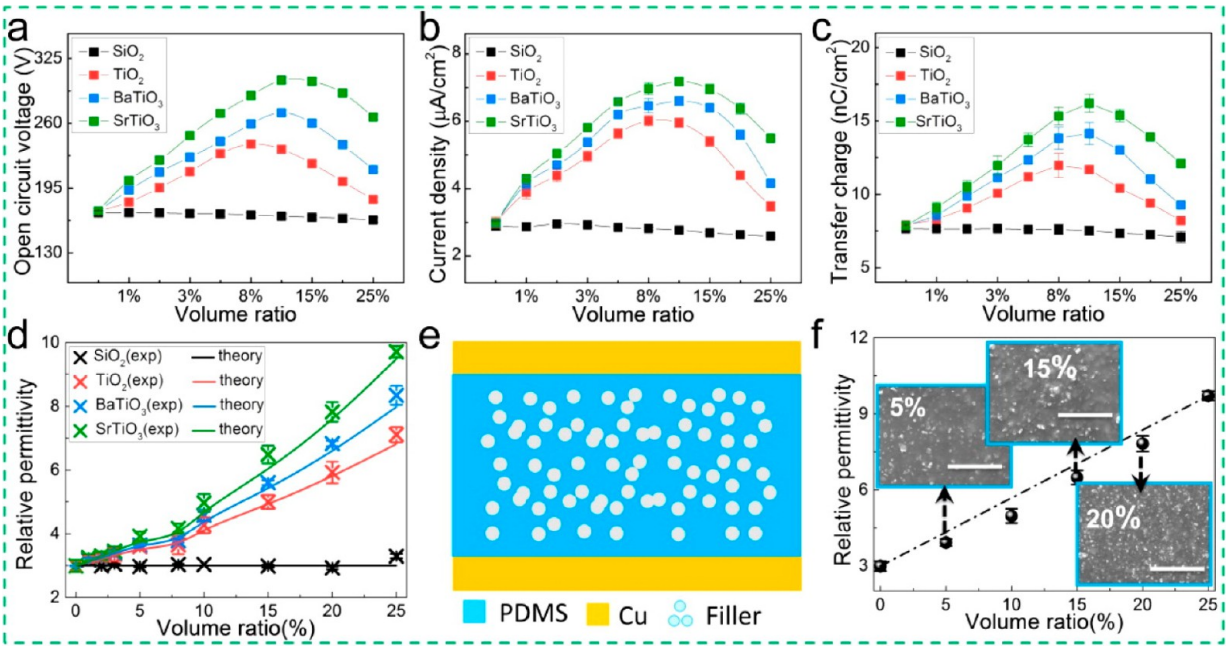

Figure 9. Electrical measurements of each as-fabricated film-based TENG (f = 2.5 Hz). (a) Open-circuit voltage, (b) short-current density, and (c) transfer charge of the $SiO_2/TiO_2/BaTiO_3/SrTiO_3$-filled samples with various volume ratios. (d) Comparison of the measured results with effective medium theoretical calculations. (e) Schematic diagram of the composite film. (f) Relative permittivity changes as a function of $SrTiO_3$ content from 0 to 25 vol %. The insets show SEM images of composite films at various volume ratios. The scale bars are 1 μm. Reproduced from ref 123. Copyright 2016 American Chemical Society.

Ba^{2+} doping showed a power density of 3.07 W/m^2, short current density of 22.8 mA/m^2, and open-circuit voltage of 200 V.

A recent study has shown that the halogen elements in perovskites can be tuned to change their polarizabilities. The polarizability of $CsPbBr_3$ is calculated at 0.47 using density function theory calculations, while it is 0.52 for $CsPbCl_3$.[128] Spontaneous polarization of the perovskites could further enhance their built-in electric field, which could lately improve the triboelectrostatic electric field by retaining more triboelectric surface charges.

3.4.2. Lead-Free Perovskite/Ferroelectric Materials. In many reports, lead-free perovskites are referred to as ferroelectric materials instead. Therefore, we use ferroelectric herewith.

Ferroelectric materials such as $BaTiO_3$ exhibit spontaneous electric polarization that can be reversed by an external electric field. Spontaneous polarization gives the material an excellent pyroelectric effect that can be used in energy harvesting for different applications.[129,130]

The application of ferroelectric materials in TENGs has recently gained increasing interest from researchers. In most studies, ferroelectric materials are composited with a polymer to form a triboelectric layer. The first application of such a layer in TENGs was reported in 2015,[123] where $BaTiO_3$ (<100 nm) and $SrTiO_3$ (<100 nm) nanoparticles were filled into sponge PDMS films (Figure 9). The high permittivity and the nanopores created by the nanoparticles resulted in enhanced performance of the TENG ($SrTiO_3$ filled) with a charge density of ~19 nC/cm^2, a maximum open-circuit voltage of 338 V, and a maximum power density of 0.647 mW/cm^2. The $BaTiO_3$-filled PMDS film yielded a charge density of ~14.7 nC/cm^2 at a volume ratio of 10%. In another report[131] in which 120 nm sized $BaTiO_3$ nanoparticles were used to fill a PDMS film, the optimized volume ratio was 30%. An output power density of 0.14 mW/cm^2 was obtained on the TENG. For composites with PVDF,[132] the optimized ratio of $BaTiO_3$ was 11.25%, which led to an open-circuit voltage of 131 V and a short-circuit current density of 89 μC/m^2. The performance was further boosted to 161 V and 112 μC/m^2 by reducing the composite layer thickness down to 5 μm. A more complex composite created by core–shell structured $BaTiO_3$–poly(*tert*-butyl acrylate) nanoparticles and PVDF[133] has also been studied as a triboelectric material. The composite has a higher dielectric constant of 26.5 at 150 MV/m, which contributes to the high output of the TENG, which is 2.5 times higher than that of the pure PVDF-based TENG.

In addition to engineering polymers, $BaTiO_3$ has also been composited with natural polymers such as cellulose for use in TENGs. Through simple vacuum filtration, $BaTiO_3$ particles can be tracked among the cellulose fibers forming a composite film.[134] The presence of the $BaTiO_3$ particles increased the dielectric constant of the cellulose film, which improved the performance of the TENG assembled with the composite film. The optimized ratio of $BaTiO_3$ particles was 13.5%, which yielded an open-circuit voltage of 181 V, short-circuit current of 21 μA, and power density of 4.8 W/m^2. The open-circuit voltage and the short-circuit current were enhanced by 150% and 310%, respectively. The addition of silver nanowires to cellulose–$BaTiO_3$ composites[135] could increase the conductivity of the composite film and could be used as both a triboelectric layer and an electrode. Simple poling treatment of the composite can further promote the TENG performance. An output power density of 180 μW/cm^2 was achieved with the film paired with fluorinated ethylene propylene (FEP). Moreover, long-term stability was realized on the TENG with no output reduction after 10 000 cycles. A similar enhancement of poling has also been found in a $BaTiO_3$/PDMS-composited triboelectric film.[131] Recently, a type of cellulose/

https://doi.org/10.1021/acsnanoscienceau.1c00026
ACS Nanosci. Au 2022, 2, 12–31

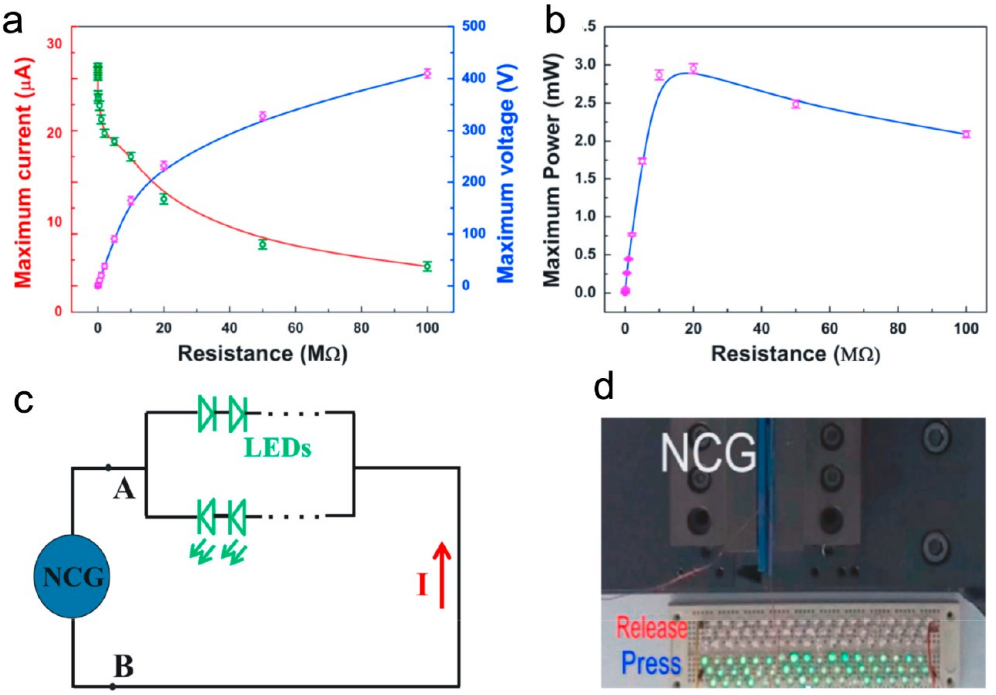

Figure 10. $ZnSnO_3$ nanocube−PDMS-composited TENG. (a) Measured load voltage and current under outer variable resistance from 10 Ω to 600 MΩ. (b) Relationship between the instantaneous power outputs and load resistance. The effective power was harvested up to 3 mW at a load resistance of ∼20 MΩ. Circuit diagram (c) and photograph (d) of blue LEDs being lit that are powered directly by the TENG. Reproduced from ref 140. Copyright 2015 Elsevier.

Table 5. Performances of Perovskite and Ferroelectric Nanomaterial Constituted TENGs

perovskite/ferroelectric nanomaterials	counter tribolayer	voltage (V)	current	power	ref
$MAPbI_3$	PTFE	22.8	0.92 μA	12.5 μW	122
$CsPbBr_3$	PVDF	240	4.13 μA/cm^2	3.31 W/m^2	124
$CsPbBr_{2.6}I_{0.4}$	PVDF	192	16.7 μA	1.2 W/m^2	125
Co(OH)(CO3)0.5/Pt/CsPbIBr2	PVDF	243	3.1 μA/cm^2	2.04 W/m^2	126
Ba^{2+} doped $CsPbBr_3$	PVDF	220	22.8 mA/m^2	3.07 W/m^2	127
$CsPbCl_3$	PVDF	258	30 μA[a]	3.06 W/m^2	128
$BaTiO_3$/PDMS	Al	375	6 μA	2.25 mW	131
$BaTiO_3$/PVDF	Nylon	161	6.2 μA	225.6 mW/m^2	132
$BaTiO_3$−P*t*BA	Al	35[a]	2.1 μA/cm^2	224 mW/m^2	133
BC/$BaTiO_3$	PDMS	181	21 μA	4.8 W/m^2	134
$BaTiO_3$/BC/Ag NWs	PTFE	460	23 μA	180 μW/cm^2	135
Cellulose/$BaTiO_3$	PDMS	88	8.3 μA	141 μW	136
PVDF−$ZnSnO_3$	PA-6	520	2.7 mA/m^2	0.47 mW/m^2	139
$ZnSnO_3$−PDMS	Al	400	7 μA/cm^2	3 mW	140

[a]Data read from the figures in the paper.

$BaTiO_3$ aerogel paper[136] was made that uses $BaTiO_3$ to increase the permittivity and charge trapping capability.

The composition of $BaTiO_3$ nanoparticles and inorganic nanomaterials has also been studied to enhance the output of TENGs. Taking advantage of the synergistic effect of multiwalled carbon nanotubes and 70 nm sized $BaTiO_3$ nanoparticles,[137] the charge and power density of a TENG was boosted to 160 μC/m^2 and 204 μW/cm^2. Larger sized $BaTiO_3$ particles (500 nm) lead to lower output, which indicates that the larger surface area of the nanoparticles plays an important role in the output enhancement. The reason for the size effect is that the smaller nanoparticles create a larger interfacial volume fraction between $BaTiO_3$ and PDMS.

Researchers have also studied other ferroelectric materials, such as $BiFeO_3$ and $ZnSnO_3$. A film made of a $BiFeO_3$-modified glass fiber fabric on a PDMS[138] layer has been studied as a triboelectric material for use in wearable hybrid nanogenerators. The nanogenerator can generate an open-circuit voltage of 110 V and a short-current density of 3.67 μA/cm^2 at a low frequency of 1 Hz. The addition of $BiFeO_3$ increased the dielectric constant from approximately 2.75 to 4, which led to an output power density of 151.42 μW/cm^2. Such a power output is based not only on the triboelectricity of the layer but also on the piezoelectricity. A similar approach has also been applied for $ZnSnO_3$ constituted TENGs,[139] where a piezoelectric membrane of PVDF−$ZnSnO_3$ and PA6 has been used as a triboelectric layer. The composite shows a piezoelectric coefficient d_{33} of −65 pm/V, which is significantly higher than that of the pure PVDF film. With the enhancement from the piezoelectric effect, the TENG made of the composite

https://doi.org/10.1021/acsnanoscienceau.1c00026
ACS Nanosci. Au 2022, 2, 12−31

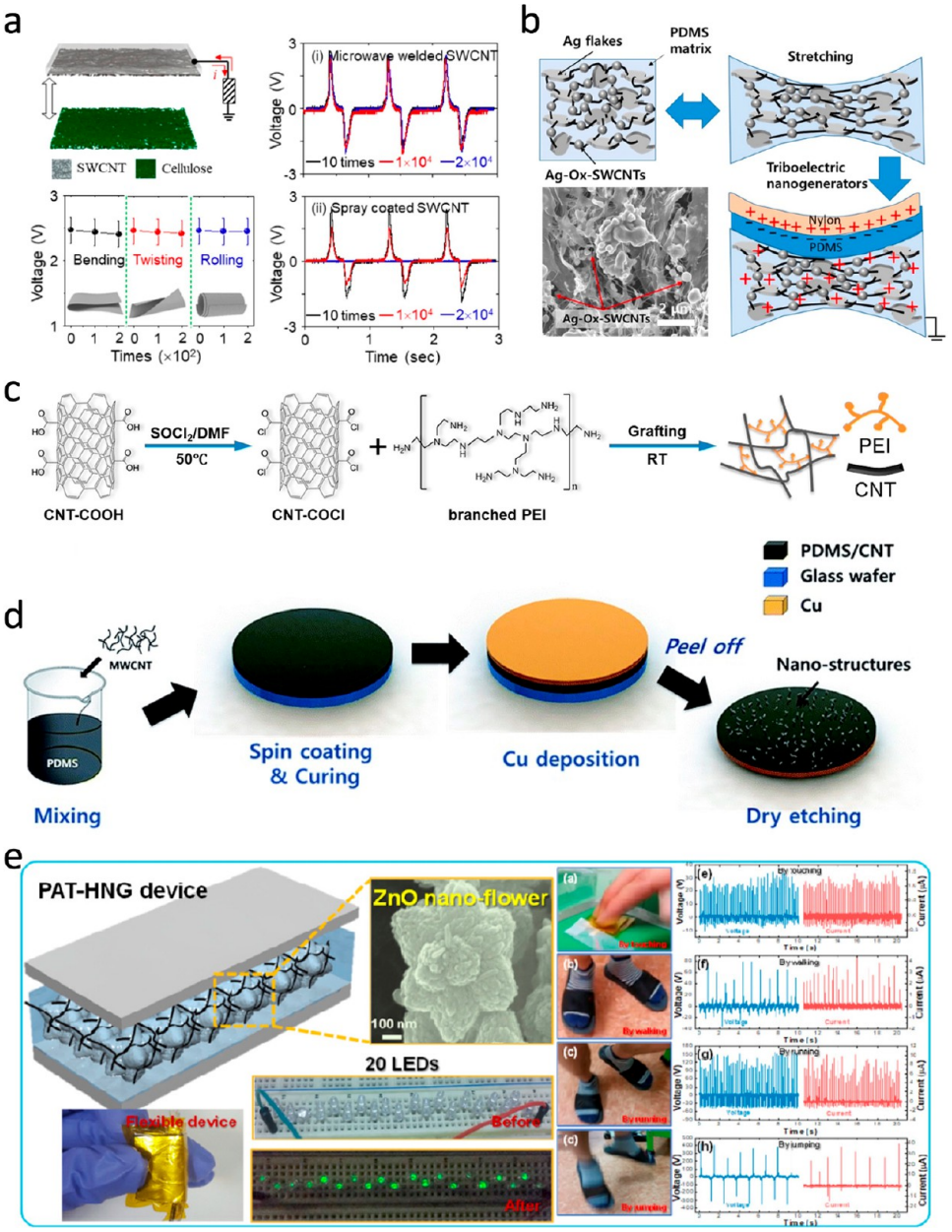

Figure 11. CNT constituted TENGs. (a) TENG with a welded SWCNT electrode. Reproduced from ref 146. Copyright 2019 Elsevier. (b) Stretchable TENG. Reproduced from ref 147. Copyright 2021 Elsevier, (c) Cross-link of CNT and PEI. Reproduced from ref 148. Copyright 2021 American Chemical Society, (d) Compositing of CNTs with PDMS. Reference 149, reused under CC BY 3.0. (e) PAT-HNG. Reproduced from ref 67. Copyright 2018 American Chemical Society.

film generated a maximum open-circuit voltage of 520 V and a short-circuit current density of 2.7 mA/m^2. Another report (Figure 10) that uses smaller $ZnSnO_3$ nanocubes[140] showed a higher short-circuit density of 7 μA/cm^2 and output power of 3 mW. Such an output can easily drive 106 blue LEDs. Mechanisms of the higher output have been suggested from the designed macrostructures and controlled microdielectric materials of the TENG.

Table 5 shows the summary of the performances of the perovskite- or ferroelectric nanomaterial constituted TENGs.

3.5. Carbon Nanomaterials

Carbon nanomaterials exist in different crystal structures and different dimensions and have different electric and dielectric properties. Therefore, the application of carbon nanomaterials in TENGs can vary based on the properties that have been utilized. Carbon nanomaterials can be amorphous or crystalline depending on their chemical structures. Carbon black is one of the typical amorphous carbons. Crystalline carbon includes graphene, graphite, carbon nanotubes, fullerenes, and diamonds.

Graphene and graphene oxide as 2D nanomaterials have been reviewed above and are excluded in this section. However, graphene quantum dots as 0D nanomaterials are included in this section. Graphite, as an important member of the carbon material family, is also reviewed here for its application in TENGs, although it is generally not considered a nanomaterial.

3.5.1. Amorphous Carbon. Amorphous carbon is usually produced by using flame methods that result in powders

https://doi.org/10.1021/acsnanoscienceau.1c00026
ACS Nanosci. Au 2022, 2, 12−31

containing nanosized carbon particles. High-temperature carbonization has also been used for producing amorphous carbon.[141] Amorphous carbon can be directly deposited on a p-type Si wafer for use as a triboelectric layer[142] that has resulted in an open-circuit voltage of 8.5 V, a short-circuit current density of 0.24 μA/cm^2, a power density of 0.5 mW/cm^2, and an instantaneous energy conversion efficiency of 7.71%. The output was further enhanced by embedding graphene sheets in the amorphous carbon layer. The embedded graphene sheets contribute two effects: an edge effect that can capture electrons and a channel effect that enhances the electron mobility in the layer. Such contribution has enhanced the output to 13.5 V, 0.35 μA/cm^2, 0.63 mW/cm^2, and 8.61%.

Carbon black is characterized under an electron microscope as nanosized particles. The materials can contain more than 97% amorphous carbon that has a high surface-area-to-volume ratio as well as good electric conductivity. Carbon black is usually composited with another material to form a triboelectric film. The presence of carbon black can change the permittivity[143] and the work function[61] of the composited film. When composited with PDMS, the charge storage characteristics of a TENG can be improved because the composite can store dynamically inserted negative charges. Such an improvement can further lead to a long-term increase in electrical charges. The content of carbon black in the composite has been experimentally found to be important since it plays a role in trapping charges. The carbon black content of 1 wt % resulted in the best performance of the TENG: 235 V, 35.6 μA/cm^2, and 0.133 mW/cm^2. Physically mixed carbon black, ZnO nanorods, and PTFE have been used to coat nickel foams for use in TENGs.[61] Carbon black, in this case, can affect the work function of ZnO nanorods because conductive electrons can transfer from carbon black to ZnO. The optimized content of carbon black here was 20 wt %, which led to an open-circuit voltage of 28 V, a short-circuit current density of 4.5 μA/cm^2, and a power density of 80 μW/cm^2.

3.5.2. Graphene Quantum Dots. Graphene quantum dots (GQDs) are nanosized layered carbon structures that have many activated parts due to dangling bonds at the edge. Such dangling bonds allow the GQDs to bind to organic and inorganic structures.

The addition of GQDs to a silver nanowire network can significantly enhance electron transfer.[144] The mechanism of the enhancement is that the electron flows to the GQDs and then to the PDMS. Such an intermediation by the GQDs reduces the barrier caused by the band mismatch of the silver and the PDMS. The enhancement of the GQDs increased the sensitivity of the triboelectric electronic skin 3 times.

GQDs can be doped and embedded in PVDF to make composite nanofibers using an electrospun technique.[145] Nitrogen-doped GQDs are negatively charged and can form ion−dipole interactions with the positive $-CH_2$ dipoles in the PVDF chains. A content of 5% GQDs in the composite fibers produces the highest output of 2.7 μW/cm^2.

3.5.3. Carbon Nanotubes. Carbon nanotubes (CNTs) are 1D carbon nanomaterials that include single-walled, double-walled, and multiwalled carbon nanotubes.

A single-walled CNT (SWCNT) network layer has been used as a p-type semiconductor to form a metal−semiconductor junction[150] with an aluminum electrode. Such a junction can reduce the loss of triboelectric charge because the SWCNT layer acts as a hole transporting layer that affects the triboelectric charge separation. The presence of the SWCNT layer can improve the charge-repelling force and the hole-blocking barrier at the interface. A wearable TENG was made based on the structure that achieved an output voltage of ∼760 V, a current of ∼51 μA, and a power density of 0.77 mW/cm^2. The SWCNT network layer has also been used directly as an electrode.[151] However, the loss of contact among the nanowires may cause the loss of conductivity during the operation. A microwave-assisted welding process can fix SWCNTs on a polycarbonate film (Figure 11a) and can significantly enhance the stability of the electrode.[146] The stability allows the electrode to be used on flexible substrates for harvesting energy. For using SWCNT-based electrodes in cases where stretchability is required, a simple compositing process has been used to create a stretchable electrode together with silver flakes and PDMS (Figure 11b).[147] A stretchable TENG working in the freestanding triboelectric layer mode was made with the electrode showing a peak power density of 84.4 mW/cm^2.

Multiwalled CNTs (MWCNTs) have been more popularly used than SWCNTs because they have electrical properties similar to those of SWCNTs but at a lower cost. MWCNTs have been used either as a form of pure layer or as a type of composite. The deposition of a MWCNT layer can enhance the contact area of the triboelectric interface.[152,153] Such an effect, plus the positive surface of the MWCNTs, can enhance triboelectric charge generation. The synergistic effects enhanced the output by a factor of 7-fold. By screen printing a layer of MWCNTs on a thermoplastic polyurethane nanofiber membrane (TPUNM), a type of stretchable TENG[154] has been made where the MWCNTs act as both an electrode material and a triboelectric layer. A maximum voltage of 218 V, a current density of 0.75 μA/cm^2, and a power density of 22.5 mW/cm^2 were obtained on the TENG by dip coating CNTs on a fiber with a silver nanowire network layer.

Using the surface chemistry of MWCNTs, cross-linked structures of MWCNTs and other materials, such as PEI (Figure 11c), have been fabricated.[148] The introduction of amide groups from PEI increases the tribopositivity, which further enhances charge transfer during the triboelectrification process. The results of the enhancements are represented by a 10-fold improvement in the output voltage and current.

Instead of chemical treatment of the MWCNTs for functionalization, direct mixing of the MWCNTs with polymers is less specific but more convenient experimentally. A MWCNT/PDMS composite can be simply produced by mixing the MWCNTs in PDMS kits (Figure 11d).[149,155,156] The addition of nanoflower-like ZnO (Figure 11e)[67] to the composite film can take advantage of the piezoelectric properties of ZnO to boost the output of a hybrid nanogenerator, namely, PAT-HNG. By mixing MWCNTs with PVA and PDAP, which resulted in dual responsive hydrogels,[39] self-healable and deformable TENGs have been fabricated that can survive under 200% strain. The mixing of ureidopyrimidinone-functionalized MWCNTs with IU-PAM could also produce self-healable TENGs.[38] By compositing with PANI, a PANI-MWCNT film-based TENG[157] could sense ammonia gas with a detection limit of 0.01 ppm.

3.5.4. Graphite. Graphite is generally not considered a nanomaterial, although nanosized graphite materials have been widely used. Here, we review the use of graphite in TENGs because the material has great importance in several aspects,

https://doi.org/10.1021/acsnanoscienceau.1c00026
ACS Nanosci. Au 2022, 2, 12−31

such as a nonmetal electrode material, an environmentally friendly material, a low-cost material, and an oxidation resist material.

In most cases, graphite is used as the electrode material. As an electrode material,[159] a thick graphite film has excellent conductivity and mechanical strength that in practice could be directly used as an electrode that can allow the TENG to have the same or even better performance than metallic electrodes. A fully green TENG (FG-TENG)[158] using only graphite as the electrode material has been reported recently. The output power of the FG-TENG using the graphite electrodes was 35% higher than that using the copper electrode (Figure 12). A thin

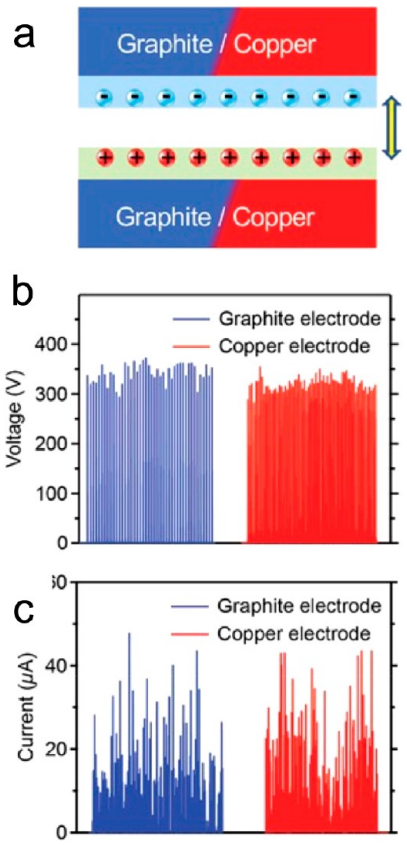

Figure 12. (a) Schematic drawing of an evaluation that compares the graphite electrodes used in the FG-TENG and copper electrodes. (b) Voltage measured on the two TENGs using graphite or copper electrodes. (c) Current measured on the two TENGs using graphite or copper electrodes. Reference 158, adapted and reused under CC BY 4.0.

graphite layer could also be coated on other substrates, such as sandpaper,[160] pristine paper,[161] and paper cards,[162] with coating methods of brushing, rod coating, and drawing, respectively.

In addition to its role as an electrode, graphite has also been composited with PDMS to form triboelectric layers for use in TENGs.[163,164] A graphite to PDMS ratio of 2:5 could result in the highest output of the TENG,[150] where the maximum open-circuit voltage is 410 V and the short-circuit current is 42 μA.

3.5.5. Other Carbon Nanomaterials. In addition to the above reviewed carbon materials, other carbon nanomaterials, such as fullerene[165] and diamond-like carbon,[166,167] have also been applied in TENG studies. The high electron affinity of the fullerene[165] could enhance the output of the TENG to a maximum open-circuit voltage of ≈1.6 kV, a short-circuit current of ≈100 μA, and a power density of 38 W/cm^2. A TENG made of a diamond-like carbon film[153] had a maximum open-circuit voltage of 38 V, a short-circuit current of 3.5 μA, and a power density of 57 mW/cm^2.

There are also studies on 3D-structured carbon nanomaterial-based TENGs that enrich the application of carbon nanomaterials. A rubber/carbon nanofiber-composited 3D structure[168] was produced and applied as a TENG operating in single electrode mode with an open-circuit voltage of 91 V and a short-circuit current of 2.87 μA. By using the templating method, patterned 3D carbon electrodes[169] have been made with the aim of increasing the contact area with the counter triboelectric layers. Compared to metallic electrodes, 3D carbon electrodes have shown more robustness to humidity and mechanical frictions.

4. CONCLUSIONS AND PERSPECTIVES

The applications of TENGs include energy harvesting, a variety of sensor types, biomedical applications, the Internet of Things (IoT), and human−computer interactions. Different applications have different requirements for the materials and production technologies.[170,171] For example, a wearable TENG requires flexible materials. Many of the requirements could not be fulfilled by macroscale materials but by nanosized materials. Therefore, different types of nanomaterials have been studied to determine their applications in TENGs. The utilization of inorganic nanomaterials in TENGs has been proven very successful. The benefits of inorganic nanomaterials include the following:

(1) Increase the contact area of the triboelectric surfaces. The high surface area to volume ratio significantly increases the contact area.

(2) Tune the dielectric properties of the composited triboelectric materials. Inorganic nanomaterials include many types of materials with dielectric properties, such as dielectric constants, spread in a very large range. By selecting the type, size, and content of the inorganic nanomaterials, the dielectric properties of the triboelectric materials could be tuned as expected.

(3) Enhance the charge transportation. The interface between a triboelectric material and an electrode may have a barrier due to the misalignment of the band structure. The presence of the nanomaterials could reduce the barrier so that the charges could be transported more conveniently.

(4) Tune the optical properties of the TENGs. Networks of nanowires such as silver and CNT nanowires can be used to fabricate transparent electrodes for use in TENGs.

(5) Mechanical properties: flexibility and stretchability. The network structures of the nanowires enabled the triboelectric films to be flexible and stretchable but retained their electrical properties.

(6) Hybrid nanogenerators. Some inorganic nanomaterials, such as ferroelectric nanomaterials, have piezoelectric properties that allow the fabrication of hybrid nanogenerators.

Although many works reviewed here have explored the advances of inorganic nanomaterials in TENGs, there are still some issues that need to be addressed in the future:

https://doi.org/10.1021/acsnanoscienceau.1c00026
ACS Nanosci. Au 2022, 2, 12−31

(1) Quantitative understanding of the relationship between the performances of the TENGs and the sizes of the inorganic nanomaterials. Theoretical models need to be developed and optimized in the future.
(2) Theoretical models of how the size and percentage of inorganic nanomaterials change the dielectric properties of the composites.
(3) Applications of new types of inorganic nanomaterials[172] in TENGs. Only a small portion of inorganic nanomaterials have been studied in the last several years, requiring more effort.

In summary, we have reviewed the recent advances of inorganic nanomaterials in triboelectric nanogenerators based on the roles, types, and characteristics of nanomaterials. The advantages of inorganic nanomaterials and the performance of TENGs promoted by inorganic nanomaterials have been reviewed. Some prospective studies have been suggested that could inspire future research in the area. This Review provides an overview of how and why inorganic nanomaterials are utilized in TENGs, which offers guidance for future studies.

AUTHOR INFORMATION

Corresponding Author

Renyun Zhang − *Department of Natural Sciences, Mid Sweden University, SE85170 Sundsvall, Sweden;* orcid.org/0000-0003-2873-7875; Email: renyun.zhang@miun.se

Author

Håkan Olin − *Department of Natural Sciences, Mid Sweden University, SE85170 Sundsvall, Sweden*

Complete contact information is available at: https://pubs.acs.org/10.1021/acsnanoscienceau.1c00026

Author Contributions

R.Z. wrote and edited the manuscript. H.O. read and edited the manuscript.

Funding

This work is financially supported by the European Regional Development Fund, the Energy Agency of Sweden, Stiftelsen Promobilia, Region Västernorrland, Sundsvalls Kommun, Timrå Kommun, and Härnösands Kommun.

Notes

The authors declare no competing financial interest.

ABBREVIATIONS

TENG, triboelectric nanogenerator; NW, nanowire; CVD, chemical vapor deposition; PDMS, polydimethylsiloxane; PEDOT:PSS, poly(3,4-ethylenedioxythiophene) polystyrenesulfonate; PTFE, polytetrafluoroethylene; PVDF, polyvinylidene fluoride; PVA, poly(vinyl alcohol); PDAP, photothermally active polydopamine particles; IU-PAM, imine bond and UPy unit, −polyazomethine; ITO, indium tin oxide; SEM, scanning electron microscope; TEM, transmission electron microscope; KPFM, Kelvin probe force microscope; CNT, carbon nanotube; SWCNT, single-walled carbon nanotube; MWCNT, multiwalled carbon nanotube; GO, graphene oxide; rGO, reduced graphene oxide; IoT, Internet of things; GQD, graphene quantum dots; PA-6, polyamide 6; PtBA, poly(*tert*-butyl acrylate); BC, bacterial cellulose

REFERENCES

(1) Fan, F.-R.; Tian, Z.-Q.; Wang, Z. L. Flexible Triboelectric Generator. *Nano Energy* **2012**, *1* (2), 328−334.
(2) Wang, Z. L.; Wang, A. C. On the Origin of Conraftact-Electrification. *Mater. Today* **2019**, *30*, 34−51.
(3) Shi, Q.; He, T.; Lee, C. More than Energy Harvesting − Combining Triboelectric Nanogenerator and Flexible Electronics Technology for Enabling Novel Micro-/Nano-Systems. *Nano Energy* **2019**, *57*, 851−871.
(4) Chen, J.; Wang, Z. L. Reviving Vibration Energy Harvesting and Self-Powered Sensing by a Triboelectric Nanogenerator. *Joule* **2017**, *1* (3), 480−521.
(5) Zheng, H.; Zi, Y.; He, X.; Guo, H.; Lai, Y.-C.; Wang, J.; Zhang, S. L.; Wu, C.; Cheng, G.; Wang, Z. L. Concurrent Harvesting of Ambient Energy by Hybrid Nanogenerators for Wearable Self-Powered Systems and Active Remote Sensing. *ACS Appl. Mater. Interfaces* **2018**, *10* (17), 14708−14715.
(6) Bian, J.; Wang, N.; Ma, J.; Jie, Y.; Zou, J.; Cao, X. Stretchable 3D Polymer for Simultaneously Mechanical Energy Harvesting and Biomimetic Force Sensing. *Nano Energy* **2018**, *47*, 442−450.
(7) Chen, X.; Miao, L.; Guo, H.; Chen, H.; Song, Y.; Su, Z.; Zhang, H. Waterproof and Stretchable Triboelectric Nanogenerator for Biomechanical Energy Harvesting and Self-Powered Sensing. *Appl. Phys. Lett.* **2018**, *112* (20), 203902.
(8) Jing, Q.; Zhu, G.; Wu, W.; Bai, P.; Xie, Y.; Han, R. P. S.; Wang, Z. L. Self-Powered Triboelectric Velocity Sensor for Dual-Mode Sensing of Rectified Linear and Rotary Motions. *Nano Energy* **2014**, *10*, 305−312.
(9) Pu, X.; Guo, H.; Chen, J.; Wang, X.; Xi, Y.; Hu, C.; Wang, Z. L. Eye Motion Triggered Self-Powered Mechnosensational Communication System Using Triboelectric Nanogenerator. *Sci. Adv.* **2017**, *3* (7), e1700694.
(10) Dhakar, L.; Pitchappa, P.; Tay, F. E. H.; Lee, C. An Intelligent Skin Based Self-Powered Finger Motion Sensor Integrated with Triboelectric Nanogenerator. *Nano Energy* **2016**, *19*, 532−540.
(11) Zheng, Q.; Shi, B.; Fan, F.; Wang, X.; Yan, L.; Yuan, W.; Wang, S.; Liu, H.; Li, Z.; Wang, Z. L. In Vivo Powering of Pacemaker by Breathing-Driven Implanted Triboelectric Nanogenerator. *Adv. Mater.* **2014**, *26* (33), 5851−5856.
(12) Zheng, Q.; Zhang, H.; Shi, B.; Xue, X.; Liu, Z.; Jin, Y.; Ma, Y.; Zou, Y.; Wang, X.; An, Z.; Tang, W.; Zhang, W.; Yang, F.; Liu, Y.; Lang, X.; Xu, Z.; Li, Z.; Wang, Z. L. In Vivo Self-Powered Wireless Cardiac Monitoring via Implantable Triboelectric Nanogenerator. *ACS Nano* **2016**, *10* (7), 6510−6518.
(13) Zheng, Q.; Shi, B.; Li, Z.; Wang, Z. L. Recent Progress on Piezoelectric and Triboelectric Energy Harvesters in Biomedical Systems. *Adv. Sci.* **2017**, *4* (7), 1700029.
(14) Chen, J.; Wang, Z. L. Reviving Vibration Energy Harvesting and Self-Powered Sensing by a Triboelectric Nanogenerator. *Joule* **2017**, *1* (3), 480−521.
(15) Wang, Z. L. On the First Principle Theory of Nanogenerators from Maxwell's Equations. *Nano Energy* **2020**, *68*, 104272.
(16) Wang, Z. L. On Maxwell's Displacement Current for Energy and Sensors: The Origin of Nanogenerators. *Mater. Today* **2017**, *20* (2), 74−82.
(17) Zhang, R.; Olin, H. Material Choices for Triboelectric Nanogenerators: A Critical Review. *EcoMat* **2020**, *2* (4), e12062.
(18) Khan, U.; Hinchet, R.; Ryu, H.; Kim, S.-W. Research Update: Nanogenerators for Self-Powered Autonomous Wireless Sensors. *APL Mater.* **2017**, *5* (7), 073803.
(19) Bai, L.; Li, Q.; Yang, Y.; Ling, S.; Yu, H.; Liu, S.; Li, J.; Chen, W. Biopolymer Nanofibers for Nanogenerator Development. *Research* **2021**, *2021*, 1−20.
(20) Wang, Z. L.; Chen, J.; Lin, L. Progress in Triboelectric Nanogenerators as a New Energy Technology and Self-Powered Sensors. *Energy Environ. Sci.* **2015**, *8* (8), 2250−2282.
(21) Wang, Z. L. Triboelectric Nanogenerators as New Energy Technology and Self-Powered Sensors − Principles, Problems and Perspectives. *Faraday Discuss.* **2014**, *176*, 447−458.

(22) Wang, Y.; Yang, Y.; Wang, Z. L. Triboelectric Nanogenerators as Flexible Power Sources. *npj Flex. Electron.* **2017**, *1* (1), 10.
(23) Zhang, C.; Wang, Z. L. Tribotronics—A New Field by Coupling Triboelectricity and Semiconductor. *Nano Today* **2016**, *11* (4), 521−536.
(24) Zhang, R.; Hummelgård, M.; Örtegren, J.; Olsen, M.; Andersson, H.; Yang, Y.; Zheng, H.; Olin, H. The Triboelectricity of the Human Body. *Nano Energy* **2021**, *86* (April), 106041.
(25) Pan, M.; Yuan, C.; Liang, X.; Zou, J.; Zhang, Y.; Bowen, C. Triboelectric and Piezoelectric Nanogenerators for Future Soft Robots and Machines. *iScience* **2020**, *23* (11), 101682.
(26) Dudem, B.; Kim, D. H.; Yu, J. S. Triboelectric Nanogenerators with Gold-Thin-Film-Coated Conductive Textile as Floating Electrode for Scavenging Wind Energy. *Nano Res.* **2018**, *11* (1), 101−113.
(27) Yang, Y.; Zhang, H.; Liu, R.; Wen, X.; Hou, T. C.; Wang, Z. L. Fully Enclosed Triboelectric Nanogenerators for Applications in Water and Harsh Environments. *Adv. Energy Mater.* **2013**, *3* (12), 1563−1568.
(28) Gong, S.; Schwalb, W.; Wang, Y.; Chen, Y.; Tang, Y.; Si, J.; Shirinzadeh, B.; Cheng, W. A Wearable and Highly Sensitive Pressure Sensor with Ultrathin Gold Nanowires. *Nat. Commun.* **2014**, *5*, 3132.
(29) Wen, J.; Chen, B.; Tang, W.; Jiang, T.; Zhu, L.; Xu, L.; Chen, J.; Shao, J.; Han, K.; Ma, W.; Wang, Z. L. Harsh-Environmental-Resistant Triboelectric Nanogenerator and Its Applications in Autodrive Safety Warning. *Adv. Energy Mater.* **2018**, *8* (29), 1801898.
(30) Kim, S.; Gupta, M. K.; Lee, K. Y.; Sohn, A.; Kim, T. Y.; Shin, K.-S.; Kim, D.; Kim, S. K.; Lee, K. H.; Shin, H.-J.; Kim, D.-W.; Kim, S.-W. Transparent Flexible Graphene Triboelectric Nanogenerators. *Adv. Mater.* **2014**, *26* (23), 3918−3925.
(31) Ning, C.; Dong, K.; Cheng, R.; Yi, J.; Ye, C.; Peng, X.; Sheng, F.; Jiang, Y.; Wang, Z. L. Flexible and Stretchable Fiber-Shaped Triboelectric Nanogenerators for Biomechanical Monitoring and Human-Interactive Sensing. *Adv. Funct. Mater.* **2021**, *31* (4), 2006679.
(32) Khan, S. A.; Zhang, H. L.; Xie, Y.; Gao, M.; Shah, M. A.; Qadir, A.; Lin, Y. Flexible Triboelectric Nanogenerator Based on Carbon Nanotubes for Self-Powered Weighing. *Adv. Eng. Mater.* **2017**, *19* (3), 1600710.
(33) Chen, H.; Xu, Y.; Bai, L.; Jiang, Y.; Zhang, J.; Zhao, C.; Li, T.; Yu, H.; Song, G.; Zhang, N.; Gan, Q. Crumpled Graphene Triboelectric Nanogenerators: Smaller Devices with Higher Output Performance. *Adv. Mater. Technol.* **2017**, *2* (6), 1700044.
(34) Stanford, M. G.; Li, J. T.; Chyan, Y.; Wang, Z.; Wang, W.; Tour, J. M. Laser-Induced Graphene Triboelectric Nanogenerators. *ACS Nano* **2019**, *13* (6), 7166−7174.
(35) Zhao, P.; Bhattacharya, G.; Fishlock, S. J.; Guy, J. G. M.; Kumar, A.; Tsonos, C.; Yu, Z.; Raj, S.; McLaughlin, J. A.; Luo, J.; Soin, N. Replacing the Metal Electrodes in Triboelectric Nanogenerators: High-Performance Laser-Induced Graphene Electrodes. *Nano Energy* **2020**, *75* (June), 104958.
(36) Chung, I. J.; Kim, W.; Jang, W.; Park, H. W.; Sohn, A.; Chung, K. B.; Kim, D. W.; Choi, D.; Park, Y. T. Layer-by-Layer Assembled Graphene Multilayers on Multidimensional Surfaces for Highly Durable, Scalable, and Wearable Triboelectric Nanogenerators. *J. Mater. Chem. A* **2018**, *6* (7), 3108−3115.
(37) Pace, G.; Serri, M.; Castillo, A. E. d. R.; Ansaldo, A.; Lauciello, S.; Prato, M.; Pasquale, L.; Luxa, J.; Mazánek, V.; Sofer, Z.; Bonaccorso, F. Nitrogen-Doped Graphene Based Triboelectric Nanogenerators. *Nano Energy* **2021**, *87* (March), 106173.
(38) Dai, X.; Huang, L.; Du, Y.; Han, J.; Zheng, Q.; Kong, J.; Hao, J. Self-Healing, Flexible, and Tailorable Triboelectric Nanogenerators for Self-Powered Sensors Based on Thermal Effect of Infrared Radiation. *Adv. Funct. Mater.* **2020**, *30* (16), 1910723.
(39) Guan, Q.; Lin, G.; Gong, Y.; Wang, J.; Tan, W.; Bao, D.; Liu, Y.; You, Z.; Sun, X.; Wen, Z.; Pan, Y. Highly Efficient Self-Healable and Dual Responsive Hydrogel-Based Deformable Triboelectric Nanogenerators for Wearable Electronics. *J. Mater. Chem. A* **2019**, *7* (23), 13948−13955.
(40) Liu, Z.; Muhammad, M.; Cheng, L.; Xie, E.; Han, W. Improved Output Performance of Triboelectric Nanogenerators Based on Polydimethylsiloxane Composites by the Capacitive Effect of Embedded Carbon Nanotubes. *Appl. Phys. Lett.* **2020**, *117* (14), 143903.
(41) Chen, H.; Bai, L.; Li, T.; Zhao, C.; Zhang, J.; Zhang, N.; Song, G.; Gan, Q.; Xu, Y. Wearable and Robust Triboelectric Nanogenerator Based on Crumpled Gold Films. *Nano Energy* **2018**, *46* (January), 73−80.
(42) Park, S.-J.; Seol, M.-L.; Jeon, S.-B.; Kim, D.; Lee, D.; Choi, Y.-K. Surface Engineering of Triboelectric Nanogenerator with an Electrodeposited Gold Nanoflower Structure. *Sci. Rep.* **2015**, *5* (1), 13866.
(43) Chun, J.; Ye, B. U.; Lee, J. W.; Choi, D.; Kang, C.-Y.; Kim, S.-W.; Wang, Z. L.; Baik, J. M. Boosted Output Performance of Triboelectric Nanogenerator via Electric Double Layer Effect. *Nat. Commun.* **2016**, *7*, 12985.
(44) Zhu, G.; Lin, Z. H.; Jing, Q.; Bai, P.; Pan, C.; Yang, Y.; Zhou, Y.; Wang, Z. L. Toward Large-Scale Energy Harvesting by a Nanoparticle-Enhanced Triboelectric Nanogenerator. *Nano Lett.* **2013**, *13* (2), 847−853.
(45) Chun, J.; Kim, J. W.; Jung, W. S.; Kang, C. Y.; Kim, S. W.; Wang, Z. L.; Baik, J. M. Mesoporous Pores Impregnated with Au Nanoparticles as Effective Dielectrics for Enhancing Triboelectric Nanogenerator Performance in Harsh Environments. *Energy Environ. Sci.* **2015**, *8* (10), 3006−3012.
(46) Lim, G.-H. H.; Kwak, S. S.; Kwon, N.; Kim, T.; Kim, H.; Kim, S.-W. W. S. M.; Kim, S.-W. W. S. M.; Lim, B. Fully Stretchable and Highly Durable Triboelectric Nanogenerators Based on Gold-Nanosheet Electrodes for Self-Powered Human-Motion Detection. *Nano Energy* **2017**, *42* (October), 300−306.
(47) Chen, B. D.; Tang, W.; Zhang, C.; Xu, L.; Zhu, L. P.; Yang, L. J.; He, C.; Chen, J.; Liu, L.; Zhou, T.; Wang, Z. L. Au Nanocomposite Enhanced Electret Film for Triboelectric Nanogenerator. *Nano Res.* **2018**, *11* (6), 3096−3105.
(48) An, T.; Anaya, D. V.; Gong, S.; Yap, L. W.; Lin, F.; Wang, R.; Yuce, M. R.; Cheng, W. Self-Powered Gold Nanowire Tattoo Triboelectric Sensors for Soft Wearable Human-Machine Interface. *Nano Energy* **2020**, *77* (July), 105295.
(49) Jiang, Q.; Chen, B.; Zhang, K.; Yang, Y. Ag Nanoparticle-Based Triboelectric Nanogenerator To Scavenge Wind Energy for a Self-Charging Power Unit. *ACS Appl. Mater. Interfaces* **2017**, *9* (50), 43716−43723.
(50) Li, W.; Sun, J.; Chen, M. Triboelectric Nanogenerator Using Nano-Ag Ink as Electrode Material. *Nano Energy* **2014**, *3*, 95−101.
(51) Zhang, R.; Engholm, M. Recent Progress on the Fabrication and Properties of Silver Nanowire-Based Transparent Electrodes. *Nanomaterials* **2018**, *8* (8), 628.
(52) Liang, X.; Zhao, T.; Jiang, W.; Yu, X.; Hu, Y.; Zhu, P.; Zheng, H.; Sun, R.; Wong, C.-P. P. Highly Transparent Triboelectric Nanogenerator Utilizing In-Situ Chemically Welded Silver Nanowire Network as Electrode for Mechanical Energy Harvesting and Body Motion Monitoring. *Nano Energy* **2019**, *59* (March), 508−516.
(53) Lee, B. Y.; Kim, S. U.; Kang, S.; Lee, S. D. Transparent and Flexible High Power Triboelectric Nanogenerator with Metallic Nanowire-Embedded Tribonegative Conducting Polymer. *Nano Energy* **2018**, *53* (June), 152−159.
(54) Jiang, Q.; Chen, B.; Yang, Y. Wind-Driven Triboelectric Nanogenerators for Scavenging Biomechanical Energy. *ACS Appl. Energy Mater.* **2018**, *1* (8), 4269−4276.
(55) Kang, H.; Kim, H.; Kim, S.; Shin, H. J.; Cheon, S.; Huh, J. H.; Lee, D. Y.; Lee, S.; Kim, S. W.; Cho, J. H. Mechanically Robust Silver Nanowires Network for Triboelectric Nanogenerators. *Adv. Funct. Mater.* **2016**, *26* (42), 7717−7724.
(56) Chen, X.; Pu, X.; Jiang, T.; Yu, A.; Xu, L.; Wang, Z. L. Tunable Optical Modulator by Coupling a Triboelectric Nanogenerator and a Dielectric Elastomer. *Adv. Funct. Mater.* **2017**, *27* (1), 1603788.
(57) Cheng, L.; Xi, Y.; Hu, C.; Yue, X.; Wang, G. Ag Nanowires Single Electrode Triboelectric Nanogenerator and Its Angle Sensors. *Energy Harvest. Syst.* **2016**, *3* (1), 91−99.

https://doi.org/10.1021/acsnanoscienceau.1c00026
ACS Nanosci. Au 2022, 2, 12−31

(58) Cheon, S.; Kang, H.; Kim, H.; Son, Y.; Lee, J. Y.; Shin, H.-J.; Kim, S.-W.; Cho, J. H. High-Performance Triboelectric Nanogenerators Based on Electrospun Polyvinylidene Fluoride-Silver Nanowire Composite Nanofibers. *Adv. Funct. Mater.* **2018**, *28* (2), 1703778.
(59) Yu, X.; Liang, X.; Krishnamoorthy, R.; Jiang, W.; Zhang, L.; Ma, L.; Zhu, P.; Hu, Y.; Sun, R.; Wong, C.-P. Transparent and Flexible Hybrid Nanogenerator with Welded Silver Nanowire Networks as the Electrodes for Mechanical Energy Harvesting and Physiological Signal Monitoring. *Smart Mater. Struct.* **2020**, *29* (4), 045040.
(60) Chen, S.-N.; Chen, C.-H.; Lin, Z.-H.; Tsao, Y.-H.; Liu, C.-P. On Enhancing Capability of Tribocharge Transfer of ZnO Nanorod Arrays by Sb Doping for Anomalous Output Performance Improvement of Triboelectric Nanogenerators. *Nano Energy* **2018**, *45*, 311−318.
(61) Jayababu, N.; Kim, D. ZnO Nanorods@conductive Carbon Black Nanocomposite Based Flexible Integrated System for Energy Conversion and Storage through Triboelectric Nanogenerator and Supercapacitor. *Nano Energy* **2021**, *82* (October), 105726.
(62) Kim, Y. J.; Lee, J.; Park, S.; Park, C.; Park, C.; Choi, H.-J. Effect of the Relative Permittivity of Oxides on the Performance of Triboelectric Nanogenerators. *RSC Adv.* **2017**, *7* (78), 49368−49373.
(63) Jeon, Y. P.; Park, J. H.; Kim, T. W. Highly Flexible Triboelectric Nanogenerators Fabricated Utilizing Active Layers with a ZnO Nanostructure on Polyethylene Naphthalate Substrates. *Appl. Surf. Sci.* **2019**, *466*, 210−214.
(64) Chen, S.-N.; Huang, M.-Z.; Lin, Z.-H.; Liu, C.-P. Enhancing Charge Transfer for ZnO Nanorods Based Triboelectric Nanogenerators through Ga Doping. *Nano Energy* **2019**, *65*, 104069.
(65) Seung, W.; Gupta, M. K.; Lee, K. Y.; Shin, K.-S.; Lee, J.-H.; Kim, T. Y.; Kim, S.; Lin, J.; Kim, J. H.; Kim, S.-W. Nanopatterned Textile-Based Wearable Triboelectric Nanogenerator. *ACS Nano* **2015**, *9* (4), 3501−3509.
(66) Ko, Y. H.; Nagaraju, G.; Lee, S. H.; Yu, J. S. PDMS-Based Triboelectric and Transparent Nanogenerators with ZnO Nanorod Arrays. *ACS Appl. Mater. Interfaces* **2014**, *6* (9), 6631−6637.
(67) Kim, D. H.; Dudem, B.; Yu, J. S. High-Performance Flexible Piezoelectric-Assisted Triboelectric Hybrid Nanogenerator via Polydimethylsiloxane-Encapsulated Nanoflower-like ZnO Composite Films for Scavenging Energy from Daily Human Activities. *ACS Sustainable Chem. Eng.* **2018**, *6* (7), 8525−8535.
(68) Jeon, Y. P.; Park, J. H.; Kim, T. W. Highly-Enhanced Triboelectric Nanogenerators Based on Zinc-Oxide Nanoripples Acting as a Triboelectric Layer. *Appl. Surf. Sci.* **2018**, *445*, 50−55.
(69) Deng, W.; Zhang, B.; Jin, L.; Chen, Y.; Chu, W.; Zhang, H.; Zhu, M.; Yang, W. Enhanced Performance of ZnO Microballoon Arrays for a Triboelectric Nanogenerator. *Nanotechnology* **2017**, *28* (13), 135401.
(70) Jakmuangpak, S.; Prada, T.; Mongkolthanaruk, W.; Harnchana, V.; Pinitsoontorn, S. Engineering Bacterial Cellulose Films by Nanocomposite Approach and Surface Modification for Biocompatible Triboelectric Nanogenerator. *ACS Appl. Electron. Mater.* **2020**, *2* (8), 2498−2506.
(71) Singh, H. H.; Khare, N. Improved Performance of Ferroelectric Nanocomposite Flexible Film Based Triboelectric Nanogenerator by Controlling Surface Morphology, Polarizability, and Hydrophobicity. *Energy* **2019**, *178*, 765−771.
(72) Pu, X.; Zha, J. W.; Zhao, C. L.; Gong, S. B.; Gao, J. F.; Li, R. K. Y. Flexible PVDF/Nylon-11 Electrospun Fibrous Membranes with Aligned ZnO Nanowires as Potential Triboelectric Nanogenerators. *Chem. Eng. J.* **2020**, *398* (30), 125526.
(73) Park, D.; Lee, S.; Anh, C. V.; Park, P.; Nah, J. Role of a Buried Indium Zinc Oxide Layer in the Performance Enhancement of Triboelectric Nanogenerators. *Nano Energy* **2019**, *55*, 501−505.
(74) Alam, M. M.; Sultana, A.; Mandal, D. Biomechanical and Acoustic Energy Harvesting from TiO2 Nanoparticle Modulated PVDF Nanofiber Made High Performance Nanogenerator. *ACS Appl. Energy Mater.* **2018**, *1* (7), 3103−3112.
(75) Park, H.-W.; Huynh, N.; Kim, W.; Hwang, H.; Hong, H.; Choi, K.; Song, A.; Chung, K.-B.; Choi, D. Effects of Embedded TiO2−x Nanoparticles on Triboelectric Nanogenerator Performance. *Micromachines* **2018**, *9* (8), 407.
(76) Bunriw, W.; Harnchana, V.; Chanthad, C.; Huynh, V. N. Natural Rubber-TiO2 Nanocomposite Film for Triboelectric Nanogenerator Application. *Polymers (Basel, Switz.)* **2021**, *13* (13), 2213.
(77) Sintusiri, J.; Harnchana, V.; Amornkitbamrung, V.; Wongsa, A.; Chindaprasirt, P. Portland Cement-TiO2 Triboelectric Nanogenerator for Robust Large-Scale Mechanical Energy Harvesting and Instantaneous Motion Sensor Applications. *Nano Energy* **2020**, *74* (January), 104802.
(78) Lin, Z. H.; Xie, Y.; Yang, Y.; Wang, S.; Zhu, G.; Wang, Z. L. Enhanced Triboelectric Nanogenerators and Triboelectric Nanosensor Using Chemically Modified TiO2 Nanomaterials. *ACS Nano* **2013**, *7* (5), 4554−4560.
(79) Park, H.-W.; Huynh, N. D.; Kim, W.; Lee, C.; Nam, Y.; Lee, S.; Chung, K.-B.; Choi, D. Electron Blocking Layer-Based Interfacial Design for Highly-Enhanced Triboelectric Nanogenerators. *Nano Energy* **2018**, *50*, 9−15.
(80) Chun, S.; Choi, I. Y.; Son, W.; Jung, J.; Lee, S.; Kim, H. S.; Pang, C.; Park, W.; Kim, J. K. High-Output and Bending-Tolerant Triboelectric Nanogenerator Based on an Interlocked Array of Surface-Functionalized Indium Tin Oxide Nanohelixes. *ACS Energy Lett.* **2019**, *4* (7), 1748−1754.
(81) Han, S. A.; Lee, K. H.; Kim, T.-H.; Seung, W.; Lee, S. K.; Choi, S.; Kumar, B.; Bhatia, R.; Shin, H.-J.; Lee, W.-J.; Kim, S.; Kim, H. S.; Choi, J.-Y.; Kim, S.-W. Hexagonal Boron Nitride Assisted Growth of Stoichiometric Al 2 O 3 Dielectric on Graphene for Triboelectric Nanogenerators. *Nano Energy* **2015**, *12*, 556−566.
(82) Im, J. S.; Park, I. K. Mechanically Robust Magnetic Fe3O4 Nanoparticle/Polyvinylidene Fluoride Composite Nanofiber and Its Application in a Triboelectric Nanogenerator. *ACS Appl. Mater. Interfaces* **2018**, *10* (30), 25660−25665.
(83) Seol, M.; Kim, S.; Cho, Y.; Byun, K.-E.; Kim, H.; Kim, J.; Kim, S. K.; Kim, S.-W.; Shin, H.-J.; Park, S. Triboelectric Series of 2D Layered Materials. *Adv. Mater.* **2018**, *30* (39), 1801210.
(84) Shankaregowda, S. A.; Nanjegowda, C. B.; Cheng, X. L.; Shi, M. Y.; Liu, Z. F.; Zhang, H. X. A Flexible and Transparent Graphene-Based Triboelectric Nanogenerator. *IEEE Trans. Nanotechnol.* **2016**, *15* (3), 435−441.
(85) Chen, H.; Xu, Y.; Zhang, J.; Wu, W.; Song, G. Enhanced Stretchable Graphene-Based Triboelectric Nanogenerator via Control of Surface Nanostructure. *Nano Energy* **2019**, *58* (September), 304−311.
(86) Xia, X.; Chen, J.; Liu, G.; Javed, M. S.; Wang, X.; Hu, C. Aligning Graphene Sheets in PDMS for Improving Output Performance of Triboelectric Nanogenerator. *Carbon* **2017**, *111*, 569−576.
(87) Kwak, S. S.; Lin, S.; Lee, J. H.; Ryu, H.; Kim, T. Y.; Zhong, H.; Chen, H.; Kim, S. W. Triboelectrification-Induced Large Electric Power Generation from a Single Moving Droplet on Graphene/Polytetrafluoroethylene. *ACS Nano* **2016**, *10* (8), 7297−7302.
(88) Zhao, X.; Chen, B.; Wei, G.; Wu, J. M.; Han, W.; Yang, Y. Polyimide/Graphene Nanocomposite Foam-Based Wind-Driven Triboelectric Nanogenerator for Self-Powered Pressure Sensor. *Adv. Mater. Technol.* **2019**, *4* (5), 1800723.
(89) Zhang, R.; Alecrim, V.; Hummelgård, M.; Andres, B.; Forsberg, S.; Andersson, M.; Olin, H. Thermally Reduced Kaolin-Graphene Oxide Nanocomposites for Gas Sensing. *Sci. Rep.* **2015**, *5*, 7676.
(90) Li, W.; Zhang, Y.; Liu, L.; Li, D.; Liao, L.; Pan, C. A High Energy Output Nanogenerator Based on Reduced Graphene Oxide. *Nanoscale* **2015**, *7* (43), 18147−18151.
(91) Wu, C.; Kim, T. W.; Choi, H. Y. Reduced Graphene-Oxide Acting as Electron-Trapping Sites in the Friction Layer for Giant Triboelectric Enhancement. *Nano Energy* **2017**, *32* (December), 542−550.
(92) Harnchana, V.; Ngoc, H. V.; He, W.; Rasheed, A.; Park, H.; Amornkitbamrung, V.; Kang, D. J. Enhanced Power Output of a Triboelectric Nanogenerator Using Poly(Dimethylsiloxane) Modified

with Graphene Oxide and Sodium Dodecyl Sulfate. *ACS Appl. Mater. Interfaces* **2018**, *10* (30), 25263−25272.
(93) Guo, H.; Li, T.; Cao, X.; Xiong, J.; Jie, Y.; Willander, M.; Cao, X.; Wang, N.; Wang, Z. L. Self-Sterilized Flexible Single-Electrode Triboelectric Nanogenerator for Energy Harvesting and Dynamic Force Sensing. *ACS Nano* **2017**, *11* (1), 856−864.
(94) Zhang, B.; Tian, G.; Xiong, D.; Yang, T.; Chun, F.; Zhong, S.; Lin, Z.; Li, W.; Yang, W. Understanding the Percolation Effect in Triboelectric Nanogenerator with Conductive Intermediate Layer. *Research* **2021**, *2021*, 7189376.
(95) Liu, Y.; Ping, J.; Ying, Y. Recent Progress in 2D-Nanomaterial-Based Triboelectric Nanogenerators. *Adv. Funct. Mater.* **2021**, *31* (17), 2009994.
(96) Gao, Y.; Liu, G.; Bu, T.; Liu, Y.; Qi, Y.; Xie, Y.; Xu, S.; Deng, W.; Yang, W.; Zhang, C. MXene Based Mechanically and Electrically Enhanced Film for Triboelectric Nanogenerator. *Nano Res.* **2021**, DOI: 10.1007/s12274-021-3437-5.
(97) Dong, Y.; Mallineni, S. S. K.; Maleski, K.; Behlow, H.; Mochalin, V. N.; Rao, A. M.; Gogotsi, Y.; Podila, R. Metallic MXenes: A New Family of Materials for Flexible Triboelectric Nanogenerators. *Nano Energy* **2018**, *44* (November), 103−110.
(98) He, W.; Sohn, M.; Ma, R.; Kang, D. J. Flexible Single-Electrode Triboelectric Nanogenerators with MXene/PDMS Composite Film for Biomechanical Motion Sensors. *Nano Energy* **2020**, *78* (September), 105383.
(99) Liu, Y.; Li, E.; Yan, Y.; Lin, Z.; Chen, Q.; Wang, X.; Shan, L.; Chen, H.; Guo, T. A One-Structure-Layer PDMS/Mxenes Based Stretchable Triboelectric Nanogenerator for Simultaneously Harvesting Mechanical and Light Energy. *Nano Energy* **2021**, *86*, 106118.
(100) Wang, D.; Lin, Y.; Hu, D.; Jiang, P.; Huang, X. Multifunctional 3D-MXene/PDMS Nanocomposites for Electrical, Thermal and Triboelectric Applications. *Composites, Part A* **2020**, *130* (December), 105754.
(101) Cai, Y.-W.; Zhang, X.-N.; Wang, G.-G.; Li, G.-Z.; Zhao, D.-Q.; Sun, N.; Li, F.; Zhang, H.-Y.; Han, J.-C.; Yang, Y. A Flexible Ultra-Sensitive Triboelectric Tactile Sensor of Wrinkled PDMS/MXene Composite Films for E-Skin. *Nano Energy* **2021**, *81*, 105663.
(102) Kim, M.; Park, D.; Alam, M. M.; Lee, S.; Park, P.; Nah, J. Remarkable Output Power Density Enhancement of Triboelectric Nanogenerators via Polarized Ferroelectric Polymers and Bulk MoS 2 Composites. *ACS Nano* **2019**, *13* (4), 4640−4646.
(103) Rana, S. M. S.; Rahman, M. T.; Salauddin, M.; Sharma, S.; Maharjan, P.; Bhatta, T.; Cho, H.; Park, C.; Park, J. Y. Electrospun PVDF-TrFE/MXene Nanofiber Mat-Based Triboelectric Nanogenerator for Smart Home Appliances. *ACS Appl. Mater. Interfaces* **2021**, *13* (4), 4955−4967.
(104) Salauddin, M.; Rana, S. M. S.; Sharifuzzaman, M.; Rahman, M. T.; Park, C.; Cho, H.; Maharjan, P.; Bhatta, T.; Park, J. Y. A Novel MXene/Ecoflex Nanocomposite-Coated Fabric as a Highly Negative and Stable Friction Layer for High-Output Triboelectric Nanogenerators. *Adv. Energy Mater.* **2021**, *11* (1), 2002832.
(105) Zhang, Z.; Yan, Q.; Liu, Z.; Zhao, X.; Wang, Z.; Sun, J.; Wang, Z. L.; Wang, R.; Li, L. Flexible MXene Composed Triboelectric Nanogenerator via Facile Vacuum-Assistant Filtration Method for Self-Powered Biomechanical Sensing. *Nano Energy* **2021**, *88*, 106257.
(106) Bhatta, T.; Maharjan, P.; Cho, H.; Park, C.; Yoon, S. H.; Sharma, S.; Salauddin, M.; Rahman, M. T.; Rana, S. S.; Park, J. Y. High-Performance Triboelectric Nanogenerator Based on MXene Functionalized Polyvinylidene Fluoride Composite Nanofibers. *Nano Energy* **2021**, *81* (November), 105670.
(107) Wang, D.; Zhang, D.; Li, P.; Yang, Z.; Mi, Q.; Yu, L. Electrospinning of Flexible Poly(Vinyl Alcohol)/MXene Nanofiber-Based Humidity Sensor Self-Powered by Monolayer Molybdenum Diselenide Piezoelectric Nanogenerator. *Nano-Micro Lett.* **2021**, *13* (1), 57.
(108) Luo, X.; Zhu, L.; Wang, Y.; Li, J.; Nie, J.; Wang, Z. L. A Flexible Multifunctional Triboelectric Nanogenerator Based on MXene/PVA Hydrogel. *Adv. Funct. Mater.* **2021**, *31*, 2104928.
(109) Jiang, C.; Wu, C.; Li, X.; Yao, Y.; Lan, L.; Zhao, F.; Ye, Z.; Ying, Y.; Ping, J. All-Electrospun Flexible Triboelectric Nanogenerator Based on Metallic MXene Nanosheets. *Nano Energy* **2019**, *59*, 268−276.
(110) Feng, Y.; He, M.; Liu, X.; Wang, W.; Yu, A.; Wan, L.; Zhai, J. Alternate-Layered MXene Composite Film-Based Triboelectric Nanogenerator with Enhanced Electrical Performance. *Nanoscale Res. Lett.* **2021**, *16* (1), 81.
(111) Cao, W.; Ouyang, H.; Xin, W.; Chao, S.; Ma, C.; Li, Z.; Chen, F.; Ma, M. A Stretchable Highoutput Triboelectric Nanogenerator Improved by MXene Liquid Electrode with High Electronegativity. *Adv. Funct. Mater.* **2020**, *30* (50), 2004181.
(112) Gallardo-Vega, C.; López-Lagunes, O.; Nava-Galindo, O. I.; De León, A.; Romero-García, J.; Aguilera-Cortés, L. A.; Martínez-Castillo, J.; Herrera-May, A. L. Triboelectric Energy Harvester Based on Stainless Steel/MoS2 and PET/ITO/PDMS for Potential Smart Healthcare Devices. *Nanomaterials* **2021**, *11* (6), 1533.
(113) Park, S.; Park, J.; Kim, Y.; Bae, S.; Kim, T.-W.; Park, K.-I.; Hong, B. H.; Jeong, C. K.; Lee, S.-K. Laser-Directed Synthesis of Strain-Induced Crumpled MoS2 Structure for Enhanced Triboelectrification toward Haptic Sensors. *Nano Energy* **2020**, *78*, 105266.
(114) Wu, C.; Kim, T. W.; Park, J. H.; An, H.; Shao, J.; Chen, X.; Wang, Z. L. Enhanced Triboelectric Nanogenerators Based on MoS 2 Monolayer Nanocomposites Acting as Electron-Acceptor Layers. *ACS Nano* **2017**, *11* (8), 8356−8363.
(115) Sahatiya, P.; Kannan, S.; Badhulika, S. Few Layer MoS2 and in Situ Poled PVDF Nanofibers on Low Cost Paper Substrate as High Performance Piezo-Triboelectric Hybrid Nanogenerator: Energy Harvesting from Handwriting and Human Touch. *Appl. Mater. Today* **2018**, *13*, 91−99.
(116) Kim, M.; Kim, S. H.; Park, M. U.; Lee, C. J.; Kim, M.; Yi, Y.; Yoo, K. H. MoS2 Triboelectric Nanogenerators Based on Depletion Layers. *Nano Energy* **2019**, *65*, 104079.
(117) Ding, R.; Wong, M.; Hao, J. Recent Advances in Hybrid Perovskite Nanogenerators. *EcoMat* **2020**, *2* (4), e12057.
(118) Ippili, S.; Jella, V.; Thomas, A. M.; Yoon, S.-G. The Recent Progress on Halide Perovskite-Based Self-Powered Sensors Enabled by Piezoelectric and Triboelectric Effects. *Nanoenergy Adv.* **2021**, *1* (1), 3−31.
(119) Sahu, M.; Hajra, S.; Bijelic, J.; Oh, D.; Djerdj, I.; Kim, H. J. Triple Perovskite-Based Triboelectric Nanogenerator: A Facile Method of Energy Harvesting and Self-Powered Information Generator. *Mater. Today Energy* **2021**, *20*, 100639.
(120) Su, L.; Zhao, Z. X.; Li, H. Y.; Yuan, J.; Wang, Z. L.; Cao, G. Z.; Zhu, G. High-Performance Organolead Halide Perovskite-Based Self-Powered Triboelectric Photodetector. *ACS Nano* **2015**, *9* (11), 11310−11316.
(121) Su, L.; Zhao, Z.; Li, H.; Wang, Y.; Kuang, S.; Cao, G.; Wang, Z.; Zhu, G. Photoinduced Enhancement of a Triboelectric Nanogenerator Based on an Organolead Halide Perovskite. *J. Mater. Chem. C* **2016**, *4* (43), 10395−10399.
(122) Yang, X.; Han, J. J.; Wang, G.; Liao, L. P.; Xu, C. Y.; Hu, W.; Li, P.; Wu, B.; Elseman, A. M.; Zhou, G. D.; Song, Q. L. Robust Perovskite-Based Triboelectric Nanogenerator Enhanced by Broadband Light and Interface Engineering. *J. Mater. Sci.* **2019**, *54* (12), 9004−9016.
(123) Chen, J.; Guo, H.; He, X.; Liu, G.; Xi, Y.; Shi, H.; Hu, C. Enhancing Performance of Triboelectric Nanogenerator by Filling High Dielectric Nanoparticles into Sponge PDMS Film. *ACS Appl. Mater. Interfaces* **2016**, *8* (1), 736−744.
(124) Wang, M.; Duan, J.; Yang, X.; Wang, Y.; Duan, Y.; Tang, Q. Interfacial Electric Field Enhanced Charge Density for Robust Triboelectric Nanogenerators by Tailoring Metal/Perovskite Schottky Junction. *Nano Energy* **2020**, *73* (March), 104747.
(125) Du, J.; Yang, X.; Duan, J.; Wang, Y.; Tang, Q. Tailoring All-Inorganic Cesium Lead Halide Perovskites for Robust Triboelectric Nanogenerators. *Nano Energy* **2020**, *70* (December), 104514.
(126) Du, J.; Duan, J.; Yang, X.; Wang, Y.; Duan, Y.; Tang, Q. Charge Boosting and Storage by Tailoring Rhombus All-Inorganic

Perovskite Nanoarrays for Robust Triboelectric Nanogenerators. *Nano Energy* **2020**, *74* (May), 104845.
(127) Wang, Y.; Duan, J.; Yang, X.; Liu, L.; Zhao, L.; Tang, Q. The Unique Dielectricity of Inorganic Perovskites toward High-Performance Triboelectric Nanogenerators. *Nano Energy* **2020**, *69* (November), 104418.
(128) Yu, X.; Liu, Z.; Yang, X.; Wang, Y.; Zhang, J.; Duan, J.; Liu, L.; Tang, Q. Crystal-Plane Controlled Spontaneous Polarization of Inorganic Perovskite toward Boosting Triboelectric Surface Charge Density. *ACS Appl. Mater. Interfaces* **2021**, *13* (22), 26196−26203.
(129) Ma, N.; Yang, Y. Enhanced Self-Powered UV Photoresponse of Ferroelectric BaTiO3Materials by Pyroelectric Effect. *Nano Energy* **2017**, *40*, 352−359.
(130) Zhao, K.; Ouyang, B.; Bowen, C. R.; Yang, Y. Enhanced Photocurrent via Ferro-Pyro-Phototronic Effect in Ferroelectric BaTiO3Materials for a Self-Powered Flexible Photodetector System. *Nano Energy* **2020**, *77*, 105152.
(131) Ali, D.; Yu, B.; Duan, X.; Yu, H.; Zhu, M. Enhancement of Output Performance through Post-Poling Technique on BaTiO 3 /PDMS-Based Triboelectric Nanogenerator. *Nanotechnology* **2017**, *28* (7), 075203.
(132) Kang, X.; Pan, C.; Chen, Y.; Pu, X. Boosting Performances of Triboelectric Nanogenerators by Optimizing Dielectric Properties and Thickness of Electrification Layer. *RSC Adv.* **2020**, *10* (30), 17752−17759.
(133) Du, X.; Liu, Y.; Wang, J.; Niu, H.; Yuan, Z.; Zhao, S.; Zhang, X.; Cao, R.; Yin, Y.; Li, N.; Zhang, C.; Xing, Y.; Xu, W.; Li, C. Improved Triboelectric Nanogenerator Output Performance through Polymer Nanocomposites Filled with Core-Shell-Structured Particles. *ACS Appl. Mater. Interfaces* **2018**, *10* (30), 25683−25688.
(134) Shao, Y.; Feng, C.; Deng, B.; Yin, B.; Yang, M. Facile Method to Enhance Output Performance of Bacterial Cellulose Nanofiber Based Triboelectric Nanogenerator by Controlling Micro-Nano Structure and Dielectric Constant. *Nano Energy* **2019**, *62*, 620−627.
(135) Oh, H.; Kwak, S. S.; Kim, B.; Han, E.; Lim, G.; Kim, S.; Lim, B. Highly Conductive Ferroelectric Cellulose Composite Papers for Efficient Triboelectric Nanogenerators. *Adv. Funct. Mater.* **2019**, *29* (37), 1904066.
(136) Shi, K.; Zou, H.; Sun, B.; Jiang, P.; He, J.; Huang, X. Dielectric Modulated Cellulose Paper/PDMS-Based Triboelectric Nanogenerators for Wireless Transmission and Electropolymerization Applications. *Adv. Funct. Mater.* **2020**, *30* (4), 1904536.
(137) Shi, K.; Sun, B.; Huang, X.; Jiang, P. Synergistic Effect of Graphene Nanosheet and BaTiO3 Nanoparticles on Performance Enhancement of Electrospun PVDF Nanofiber Mat for Flexible Piezoelectric Nanogenerators. *Nano Energy* **2018**, *52* (May), 153−162.
(138) Liu, J.; Yu, D.; Zheng, Z.; Huangfu, G.; Guo, Y. Lead-Free BiFeO3 Film on Glass Fiber Fabric: Wearable Hybrid Piezoelectric-Triboelectric Nanogenerator. *Ceram. Int.* **2021**, *47* (3), 3573−3579.
(139) Soin, N.; Zhao, P.; Prashanthi, K.; Chen, J.; Ding, P.; Zhou, E.; Shah, T.; Ray, S. C.; Tsonos, C.; Thundat, T.; Siores, E.; Luo, J. High Performance Triboelectric Nanogenerators Based on Phase-Inversion Piezoelectric Membranes of Poly(Vinylidene Fluoride)-Zinc Stannate (PVDF-ZnSnO3) and Polyamide-6 (PA6). *Nano Energy* **2016**, *30* (October), 470−480.
(140) Wang, G.; Xi, Y.; Xuan, H.; Liu, R.; Chen, X.; Cheng, L. Hybrid Nanogenerators Based on Triboelectrification of a Dielectric Composite Made of Lead-Free ZnSnO3 Nanocubes. *Nano Energy* **2015**, *18*, 28−36.
(141) Gao, S.; Chen, Y.; Su, J.; Wang, M.; Wei, X.; Jiang, T.; Wang, Z. L. Triboelectric Nanogenerator Powered Electrochemical Degradation of Organic Pollutant Using Pt-Free Carbon Materials. *ACS Nano* **2017**, *11* (4), 3965−3972.
(142) Zhang, W.; Diao, D.; Sun, K.; Fan, X.; Wang, P. Study on Friction-Electrification Coupling in Sliding-Mode Triboelectric Nanogenerator. *Nano Energy* **2018**, *48* (January), 456−463.
(143) Choi, J. H.; Ra, Y.; Cho, S.; La, M.; Park, S. J.; Choi, D. Electrical Charge Storage Effect in Carbon Based Polymer Composite for Long-Term Performance Enhancement of the Triboelectric Nanogenerator. *Compos. Sci. Technol.* **2021**, *207* (July), 108680.
(144) Xu, Z.; Wu, C.; Li, F.; Chen, W.; Guo, T.; Kim, T. W. Triboelectric Electronic-Skin Based on Graphene Quantum Dots for Application in Self-Powered, Smart, Artificial Fingers. *Nano Energy* **2018**, *49* (March), 274−282.
(145) Choi, G. J.; Baek, S. H.; Lee, S. S.; Khan, F.; Kim, J. H.; Park, I. K. Performance Enhancement of Triboelectric Nanogenerators Based on Polyvinylidene Fluoride/Graphene Quantum Dot Composite Nanofibers. *J. Alloys Compd.* **2019**, *797*, 945−951.
(146) Kim, H. S.; Kim, D. Y.; Kwak, J. H.; Kim, J. H.; Choi, M.; Hyung Kim, D.; Lee, D. W.; Kong, D. S.; Park, J.; Jung, S.; Lee, G. H.; Lee, M.; Jung, J. H. Microwave-Welded Single-Walled Carbon Nanotubes as Suitable Electrodes for Triboelectric Energy Harvesting from Biomaterials and Bioproducts. *Nano Energy* **2019**, *56* (October), 338−346.
(147) Yang, H. J.; Lee, J. W.; Seo, S. H.; Jeong, B.; Lee, B.; Do, W. J.; Kim, J. H.; Cho, J. Y.; Jo, A.; Jeong, H. J.; Jeong, S. Y.; Kim, G. H.; Lee, G. W.; Shin, Y. E.; Ko, H.; Han, J. T.; Park, J. H. Fully Stretchable Self-Charging Power Unit with Micro-Supercapacitor and Triboelectric Nanogenerator Based on Oxidized Single-Walled Carbon Nanotube/Polymer Electrodes. *Nano Energy* **2021**, *86* (February), 106083.
(148) Feng, P. Y.; Xia, Z.; Sun, B.; Jing, X.; Li, H.; Tao, X.; Mi, H. Y.; Liu, Y. Enhancing the Performance of Fabric-Based Triboelectric Nanogenerators by Structural and Chemical Modification. *ACS Appl. Mater. Interfaces* **2021**, *13* (14), 16916−16927.
(149) Kim, M.-K.; Kim, M.-S.; Kwon, H.-B.; Jo, S.-E.; Kim, Y.-J. Wearable Triboelectric Nanogenerator Using a Plasma-Etched PDMS−CNT Composite for a Physical Activity Sensor. *RSC Adv.* **2017**, *7* (76), 48368−48373.
(150) Byeong-Cheol Kang; Choi, H. J.; Park, S. J.; Ha, T. J. Wearable Triboelectric Nanogenerators with the Reduced Loss of Triboelectric Charges by Using a Hole Transport Layer of Bar-Printed Single-Wall Carbon Nanotube Random Networks. *Energy* **2021**, *233*, 121196.
(151) Zhong, J.; Zhu, H.; Zhong, Q.; Dai, J.; Li, W.; Jang, S. H.; Yao, Y.; Henderson, D.; Hu, Q.; Hu, L.; Zhou, J. Self-Powered Human-Interactive Transparent Nanopaper Systems. *ACS Nano* **2015**, *9* (7), 7399−7406.
(152) Javadi, M.; Heidari, A.; Darbari, S. Realization of Enhanced Sound-Driven CNT-Based Triboelectric Nanogenerator, Utilizing Sonic Array Configuration. *Curr. Appl. Phys.* **2018**, *18* (4), 361−368.
(153) Lu, C.; Chen, J.; Jiang, T.; Gu, G.; Tang, W.; Wang, Z. L. A Stretchable, Flexible Triboelectric Nanogenerator for Self-Powered Real-Time Motion Monitoring. *Adv. Mater. Technol.* **2018**, *3* (6), 1800021.
(154) Zhao, S.; Wang, J.; Du, X.; Wang, J.; Cao, R.; Yin, Y.; Zhang, X.; Yuan, Z.; Xing, Y.; Pui, D. Y. H.; Li, C. All-Nanofiber-Based Ultralight Stretchable Triboelectric Nanogenerator for Self-Powered Wearable Electronics. *ACS Appl. Energy Mater.* **2018**, *1* (5), 2326−2332.
(155) Rasel, M. S.; Maharjan, P.; Salauddin, M.; Rahman, M. T.; Cho, H. O.; Kim, J. W.; Park, J. Y. An Impedance Tunable and Highly Efficient Triboelectric Nanogenerator for Large-Scale, Ultra-Sensitive Pressure Sensing Applications. *Nano Energy* **2018**, *49* (March), 603−613.
(156) Wang, X.; Yang, B.; Liu, J.; Zhu, Y.; Yang, C.; He, Q. A Flexible Triboelectric-Piezoelectric Hybrid Nanogenerator Based on P(VDF-TrFE) Nanofibers and PDMS/MWCNT for Wearable Devices. *Sci. Rep.* **2016**, *6* (1), 36409.
(157) Wang, S.; Xie, G.; Tai, H.; Su, Y.; Yang, B.; Zhang, Q.; Du, X.; Jiang, Y. Ultrasensitive Flexible Self-Powered Ammonia Sensor Based on Triboelectric Nanogenerator at Room Temperature. *Nano Energy* **2018**, *51*, 231−240.
(158) Zhang, R.; Dahlström, C.; Zou, H.; Jonzon, J.; Hummelgård, M.; Örtegren, J.; Blomquist, N.; Yang, Y.; Andersson, H.; Olsen, M.; Norgren, M.; Olin, H.; Wang, Z. L. Cellulose-Based Fully Green

Triboelectric Nanogenerators with Output Power Density of 300 W m − 2. *Adv. Mater.* **2020**, *32* (38), 2002824.
(159) Lee, S. H.; Ko, Y. H.; Yu, J. S. Facile Fabrication and Characterization of Arch-Shaped Triboelectric Nanogenerator with a Graphite Top Electrode. *Phys. Status Solidi A* **2015**, *212* (2), 401−405.
(160) Ankanahalli Shankaregowda, S.; Sagade Muktar Ahmed, R. F.; Liu, Y.; Bananakere Nanjegowda, C.; Cheng, X.; Shivanna, S.; Ramakrishna, S.; Yu, Z.; Zhang, X.; Sannathammegowda, K. Dry-Coated Graphite onto Sandpaper for Triboelectric Nanogenerator as an Active Power Source for Portable Electronics. *Nanomaterials* **2019**, *9* (11), 1585.
(161) Ankanahalli Shankaregowda, S.; Sagade Muktar Ahmed, R. F.; Nanjegowda, C. B.; Wang, J.; Guan, S.; Puttaswamy, M.; Amini, A.; Zhang, Y.; Kong, D.; Sannathammegowda, K.; Wang, F.; Cheng, C. Single-Electrode Triboelectric Nanogenerator Based on Economical Graphite Coated Paper for Harvesting Waste Environmental Energy. *Nano Energy* **2019**, *66* (July), 104141.
(162) Zhang, X.-S.; Su, M.; Brugger, J.; Kim, B. Penciling a Triboelectric Nanogenerator on Paper for Autonomous Power MEMS Applications. *Nano Energy* **2017**, *33*, 393−401.
(163) Sun, Q. J.; Lei, Y.; Zhao, X. H.; Han, J.; Cao, R.; Zhang, J.; Wu, W.; Heidari, H.; Li, W. J.; Sun, Q.; Roy, V. A. L. Scalable Fabrication of Hierarchically Structured Graphite/Polydimethylsiloxane Composite Films for Large-Area Triboelectric Nanogenerators and Self-Powered Tactile Sensing. *Nano Energy* **2021**, *80* (August), 105521.
(164) Zhang, X.; He, D.; Palaniappan, V.; Maddipatla, D.; Yang, Q.; Atashbar, M. Z. A Novel Graphite/PDMS Based Flexible Triboelectric Nanogenerator. In *2021 IEEE International Conference on Flexible and Printable Sensors and Systems (FLEPS)*; IEEE, 2021; pp 1−4. DOI: 10.1109/FLEPS51544.2021.9469812.
(165) Parajuli, P.; Sharma, B.; Behlow, H.; Rao, A. M. Fullerene-Enhanced Triboelectric Nanogenerators. *Adv. Mater. Technol.* **2020**, *5* (8), 2000295.
(166) Ramaswamy, S. H.; Shimizu, J.; Chen, W.; Kondo, R.; Choi, J. Investigation of Diamond-like Carbon Films as a Promising Dielectric Material for Triboelectric Nanogenerator. *Nano Energy* **2019**, *60* (February), 875−885.
(167) Ramaswamy, S. H.; Kondo, R.; Chen, W.; Fukushima, I.; Choi, J. Development of Highly Durable Sliding Triboelectric Nanogenerator Using Diamond-like Carbon Films. *Tribol. Online* **2020**, *15* (2), 89−97.
(168) Shao, Y.; Luo, C.; Deng, B.-w.; Yin, B.; Yang, M. bo. Flexible Porous Silicone Rubber-Nanofiber Nanocomposites Generated by Supercritical Carbon Dioxide Foaming for Harvesting Mechanical Energy. *Nano Energy* **2020**, *67* (November), 104290.
(169) Kim, D.; Pramanick, B.; Salazar, A.; Tcho, I.; Madou, M. J.; Jung, E. S.; Choi, Y.; Hwang, H. 3D Carbon Electrode Based Triboelectric Nanogenerator. *Adv. Mater. Technol.* **2016**, *1* (8), 1600160.
(170) Chen, B.; Tang, W.; Wang, Z. L. Advanced 3D Printing-Based Triboelectric Nanogenerator for Mechanical Energy Harvesting and Self-Powered Sensing. *Mater. Today* **2021**, *xxx* (xx), 1−15.
(171) Chen, B.; Tang, W.; Jiang, T.; Zhu, L.; Chen, X.; He, C.; Xu, L.; Guo, H.; Lin, P.; Li, D.; Shao, J.; Wang, Z. L. Three-Dimensional Ultraflexible Triboelectric Nanogenerator Made by 3D Printing. *Nano Energy* **2018**, *45* (December), 380−389.
(172) Zhang, R.; Hummelgård, M.; Örtegren, J.; Olsen, M.; Andersson, H.; Yang, Y.; Wang, Z.; Olin, H.; Sutar, P.; Mihailovic, D. All-Inorganic Triboelectric Nanogenerators Based on Mo6S3I6 and Indium Tin Oxide. *Nano Energy* **2021**, *89* (June), 106363.

https://doi.org/10.1021/acsnanoscienceau.1c00026
ACS Nanosci. Au 2022, 2, 12−31